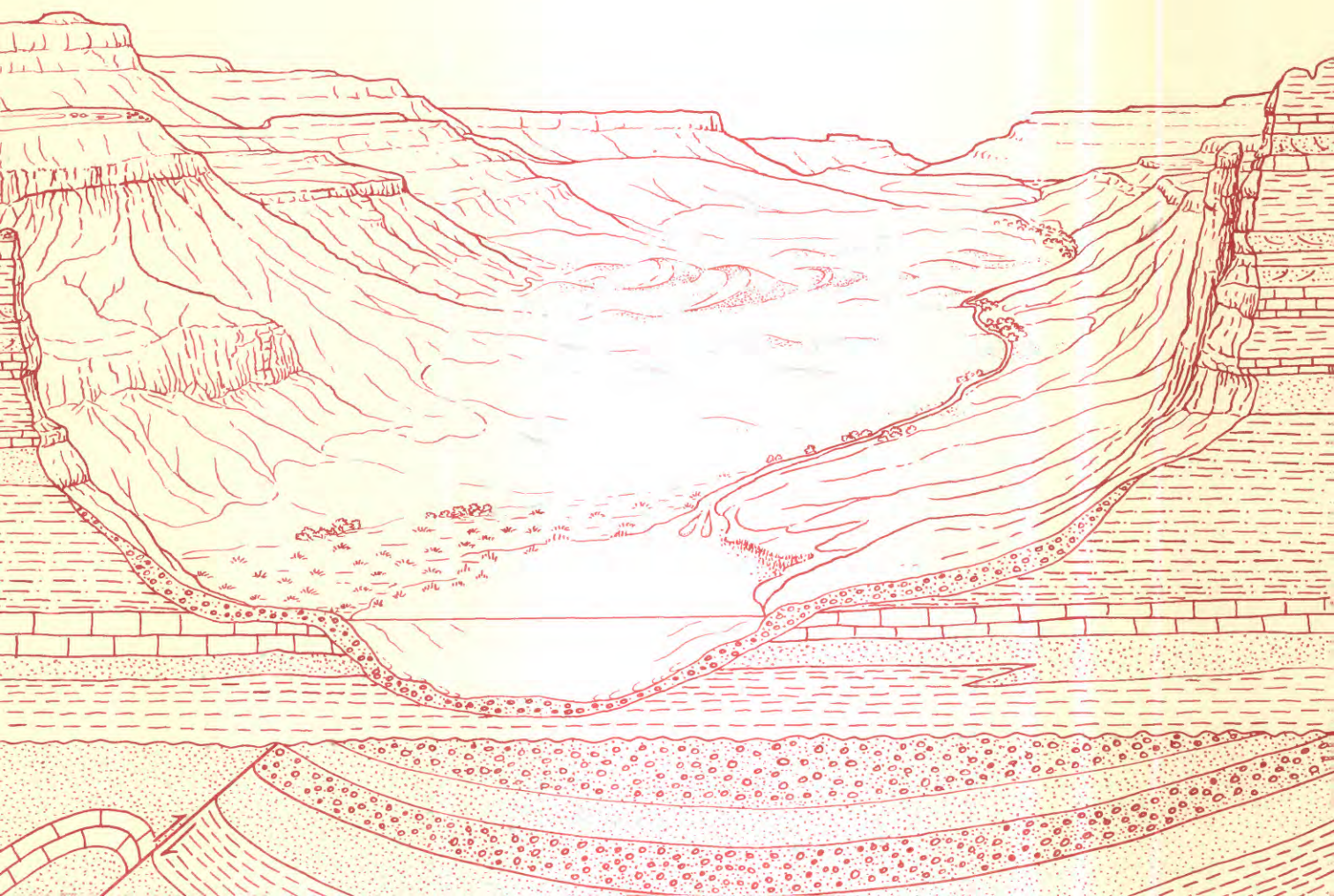


Petrography, Mineralogy, and Reservoir Characteristics of the Upper Cretaceous Mesaverde Group in the East-Central Piceance Basin, Colorado

U.S. GEOLOGICAL SURVEY BULLETIN 1787-G



Chapter G

Petrography, Mineralogy, and Reservoir Characteristics of the Upper Cretaceous Mesaverde Group in the East-Central Piceance Basin, Colorado

By JANET K. PITMAN, CHARLES W. SPENCER, and
RICHARD M. POLLASTRO

A multidisciplinary approach to research studies of
sedimentary rocks and their constituents and the
evolution of sedimentary basins, both ancient and modern

U.S. GEOLOGICAL SURVEY BULLETIN 1787

EVOLUTION OF SEDIMENTARY BASINS—UINTA AND PICEANCE BASINS

DEPARTMENT OF THE INTERIOR
MANUEL LUJAN, JR., Secretary



U. S. GEOLOGICAL SURVEY
Dallas L. Peck, Director

Any use of trade, product, or firm names in this publication is for descriptive purposes only and does not imply endorsement by the U.S. Government.

UNITED STATES GOVERNMENT PRINTING OFFICE: 1989

For sale by the
Books and Open-File Reports Section
U.S. Geological Survey
Federal Center
Box 25425
Denver, CO 80225

Library of Congress Cataloging-in-Publication Data

Pitman, Janet K.

Petrography, mineralogy, and reservoir characteristics of the Upper Cretaceous Mesaverde Group in the East-Central Piceance Basin, Colorado / by Janet K. Pitman, Charles W. Spencer, and Richard M. Pollastro.

p. cm. — (Evolution of sedimentary basins-Uinta and Piceance basins ; ch. G) (U.S. Geological Survey bulletin ; 1787-G)

Bibliography: p.

Supt. of Docs. no.: I 19.3: 1787-G

1. Geology—Colorado—Piceance Creek Watershed. 2. Gas, Natural—Colorado—Piceance Creek Watershed. 3. Mesaverde Group. 4. Geology, Stratigraphic—Cretaceous. I. Spencer, Charles Winthrop, 1930- . II. Pollastro, Richard M. III. Title. IV. Series.

V. Series: U.S. Geological Survey bulletin ; 1787-G.

QE75.B9 no. 1787-G

[QE92.P47]

557.3 s—dc20

[553.2'85'09788]

89-600022
CIP

CONTENTS

| | |
|--------------------------------------|-----|
| Abstract | G1 |
| Introduction | G1 |
| Analytical methods | G4 |
| Petrology and mineralogy | G5 |
| Mixed marine-nonmarine zone | G7 |
| Framework grains | G7 |
| Authigenic minerals | G8 |
| Reservoir properties | G10 |
| Fluvial zone | G10 |
| Framework grains | G10 |
| Authigenic minerals | G12 |
| Reservoir properties | G14 |
| Coastal zone | G15 |
| Framework grains | G15 |
| Authigenic minerals | G17 |
| Reservoir properties | G17 |
| Paludal zone | G19 |
| Framework grains | G19 |
| Authigenic minerals | G19 |
| Reservoir properties | G19 |
| Shoreline-marine zone | G23 |
| Framework grains | G23 |
| Authigenic minerals | G25 |
| Reservoir properties | G25 |
| Interpretations from clay mineralogy | G28 |
| Summary | G30 |
| References cited | G30 |

PLATE

[Plate is in pocket]

1. Mineralogic profiles for sandstones from MWX-1, MWX-2, and MWX-3 wells, east-central Piceance basin, northwestern Colorado.

FIGURES

1. Map showing location of MWX site and selected Tertiary and Upper Cretaceous gas fields, Piceance basin, western Colorado G2
2. Map showing structure contours of top of Rollins Sandstone Member of Mount Garfield of Mesaverde Group G3
3. Diagram showing relative positions of MWX wells G4
4. Diagram showing depositional zones, discrete sandstone beds, cored intervals, and individual log runs in MWX wells G5
5. Gamma-ray log profiles through MWX wells showing lateral continuity of discrete sandstone units G6
6. Ternary diagram showing mineralogic compositions of framework grains in sandstones of mixed marine-nonmarine zone G8

7. Thin-section photomicrographs showing detrital constituents, mineral cements, and dissolution features in sandstones of mixed marine-nonmarine zone **G9**
8. Ternary diagram showing mineralogic compositions of framework grains in sandstones of fluvial zone **G11**
9. Thin-section photomicrographs showing framework grains, authigenic cements, porosity, and mineralized fractures in sandstones of fluvial zone **G12**
- 10–11. Crossplots of core porosity and conventionally measured permeability for sandstones in interval:
 10. 5,505–5,855 ft in fluvial zone of MWX–2 well **G14**
 11. 5,700.5–5,846.3 ft in fluvial zone of MWX–1 well **G15**
12. Crossplot of core porosity and grain density for sandstones in interval 5,705–5,855 ft in fluvial zone of MWX–2 well **G15**
13. Ternary diagram showing mineralogic compositions of framework grains in sandstones of coastal zone **G16**
14. Thin-section photomicrographs showing detrital grains, mineral cements, and porosity in sandstones of coastal zone **G17**
15. Scanning electron photomicrograph showing pore throat filled with bridging illite and illite/smectite **G18**
16. Crossplot of core porosity and conventionally measured permeability for sandstones in coastal zone of MWX–1 well **G18**
17. Crossplot of core porosity and grain density of framework grains in sandstones of coastal zone of MWX–2 well **G18**
18. Ternary diagram showing mineralogic compositions of framework grains in sandstones of paludal zone **G20**
19. Thin-section photomicrographs showing framework grains and porosity in sandstones of paludal zone **G21**
20. Scanning electron photomicrograph showing framework quartz and carbonate cement that have been partly dissolved and replaced by authigenic clay in sandstone from paludal zone **G21**
21. Scanning electron photomicrograph showing illite and illite/smectite replacing rock fragments and bridging pore throats **G22**
22. Thin-section photomicrographs showing abundant rip-up shale and siltstone clasts reworked into enclosing sandstone beds **G22**
23. Crossplot of core porosity and core-measured grain density of sandstones in paludal zone **G22**
24. Ternary diagram showing mineralogic compositions of framework grains in sandstones of shoreline-marine zone **G23**
25. Thin-section photomicrographs showing detrital constituents, mineral cements, and dissolution features in sandstones of shoreline-marine zone **G24**
- 26–30. Scanning electron photomicrograph showing:
 26. Pore containing authigenic iron-rich chlorite **G25**
 27. Microporosity between individual silica crystals in partly dissolved chert grain **G26**
 28. Open intergranular pores between authigenic quartz crystals **G27**
 29. Fibrous and pore-bridging authigenic illite **G27**
 30. Clays and cements in sandstones **G29**

TABLES

1. Mineralogy of sandstones in MWX wells as calculated by using X-ray diffraction **G7**
2. Calculated weight percent of clay minerals $< 2 \mu\text{m}$ fraction, in sandstones and shales, MWX wells **G28**

CONVERSION FACTORS FOR SOME SI METRIC AND U.S. UNITS OF MEASURE

| To convert from | To | Multiply by |
|-------------------------|----------------------|--|
| Feet (ft) | Meters (m) | 0.3048 |
| Miles (mi) | Kilometers (km) | 1.609 |
| Pounds (lb) | Kilograms (kg) | 0.4536 |
| Degrees Fahrenheit (°F) | Degrees Celsius (°C) | $\text{Temp } ^\circ\text{C} = (\text{temp } ^\circ\text{F} - 32) / 1.8$ |

Petrography, Mineralogy, and Reservoir Characteristics of the Upper Cretaceous Mesaverde Group in the East-Central Piceance Basin, Colorado

By Janet K. Pitman, Charles W. Spencer, and Richard M. Pollastro

Abstract

Large amounts of natural gas occur in low-permeability (tight) reservoir rocks of Cretaceous age in the Piceance basin of northwest Colorado. Three closely spaced wells drilled through the Upper Cretaceous Mesaverde Group as part of the U.S. Department of Energy's Multiwell Experiment (MWX) were extensively cored and logged in order to identify the factors controlling the occurrence and distribution of gas in low-permeability rocks and to improve recovery technology. X-ray diffraction and petrographic studies reveal that potential reservoir rocks in the Mesaverde are composed of varying amounts of framework grains including quartz, feldspar, and volcanic and sedimentary lithic fragments; authigenic mineral cements including quartz and carbonate; and clay minerals including illite, mixed-layer illite/smectite, chlorite and kaolinite in the upper part of the group, and dominantly illite and illite/smectite in the lower part of the group.

Porosity and permeability of reservoir sandstones in the Mesaverde Group typically are low. Porosity is best developed in rocks that have undergone dissolution of chemically unstable lithic grains and carbonate cement and is significantly reduced in sandstones containing abundant deformed lithic grains, detrital matrix, and authigenic pore-fill carbonate cement. Permeability to gas in the Mesaverde is low (<0.1 millidarcy) because the sandstones have complex pore geometries resulting from extensive authigenic clay mineral formation in secondary pores. At in situ conditions, water adsorbed on clay surfaces creates high irreducible saturations. These high saturations result in low gas-saturated pore volumes that significantly retard fluid flow through poorly connected pores. Production-test data

indicate that production of natural gas in the MWX wells is controlled by both permeability and the distribution of natural fractures; drill cores taken through the Mesaverde in these wells display extensive open and partly mineralized natural fractures. Fracture-analysis studies and detailed mineralogic investigations are necessary to successfully explore and produce gas from these low-permeability reservoir rocks in the Piceance basin and other basins of the Rocky Mountain region.

INTRODUCTION

The Piceance basin in northwestern Colorado contains major resources of natural gas in low-permeability (tight) reservoir rocks (fig. 1). Such rocks typically have in situ permeabilities to gas of less than 0.1 millidarcy (mD). The National Petroleum Council (NPC) appraised 12 basins and areas in the United States and estimated that tight-gas reservoirs in these basins contain 444 trillion cubic feet (TCF) of gas in place, of which about 231 TCF is recoverable (NPC, 1980, p. 31). If these data are extrapolated to 101 additional basins in the United States, then 608 TCF of gas may be recoverable from tight sandstone reservoirs in 113 U.S. basins. The NPC study indicates that the Piceance basin contains no more than 32 TCF of recoverable gas in low-permeability rocks. Most gas in the Piceance basin is in fluvial and marine sandstone sequences in the Upper Cretaceous Mesaverde Group and lower Tertiary Wasatch Formation. Major gas resources also occur in tight rocks of similar age and origin in other basins in the Rocky Mountain region.

In 1981, the U.S. Department of Energy (DOE) initiated a field-oriented, enhanced-gas-recovery research experiment in the southern part of the Piceance

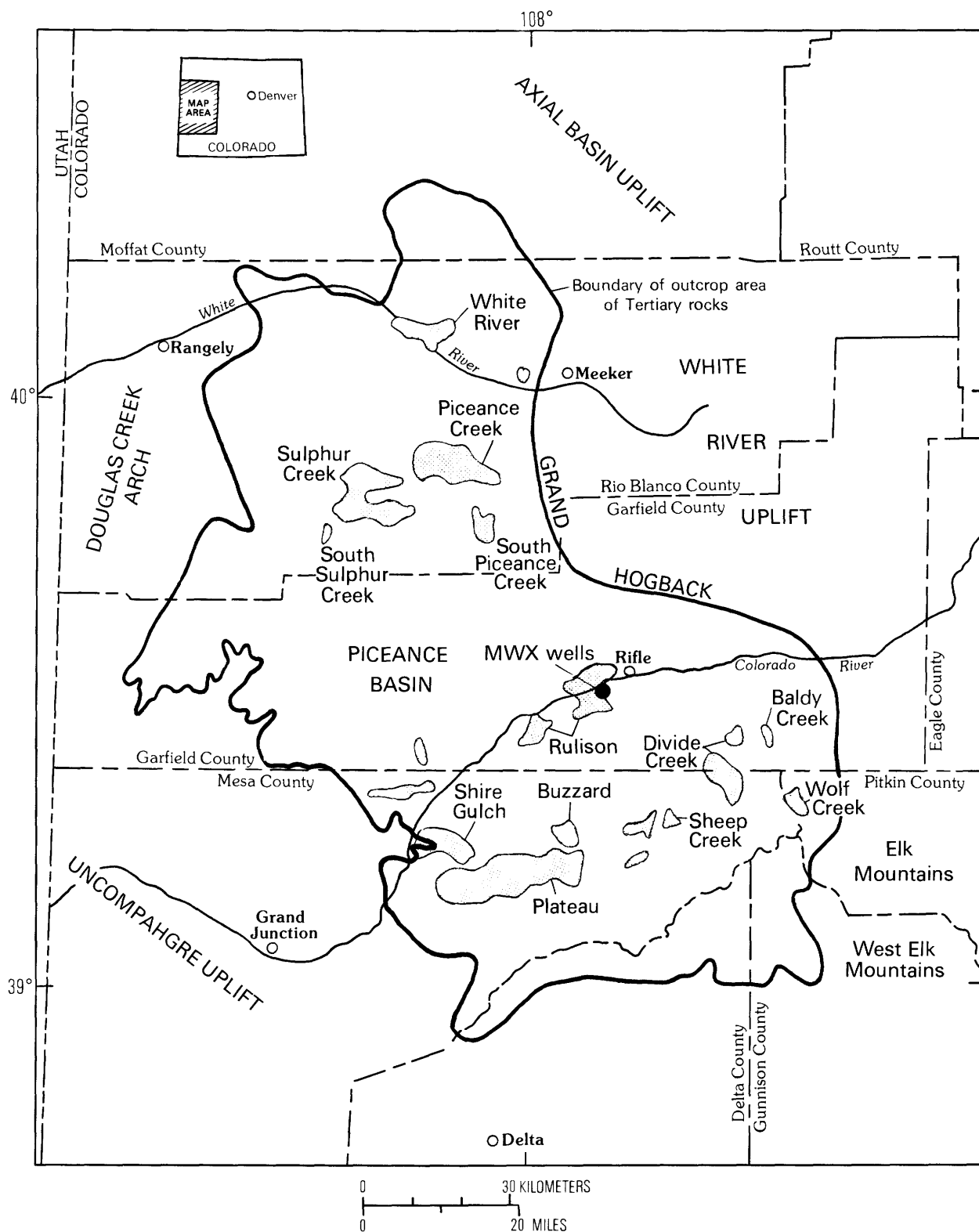


Figure 1. MWX site and selected Tertiary and Upper Cretaceous gas fields (pattern), Piceance basin, western Colorado. Modified from Dunn (1974).

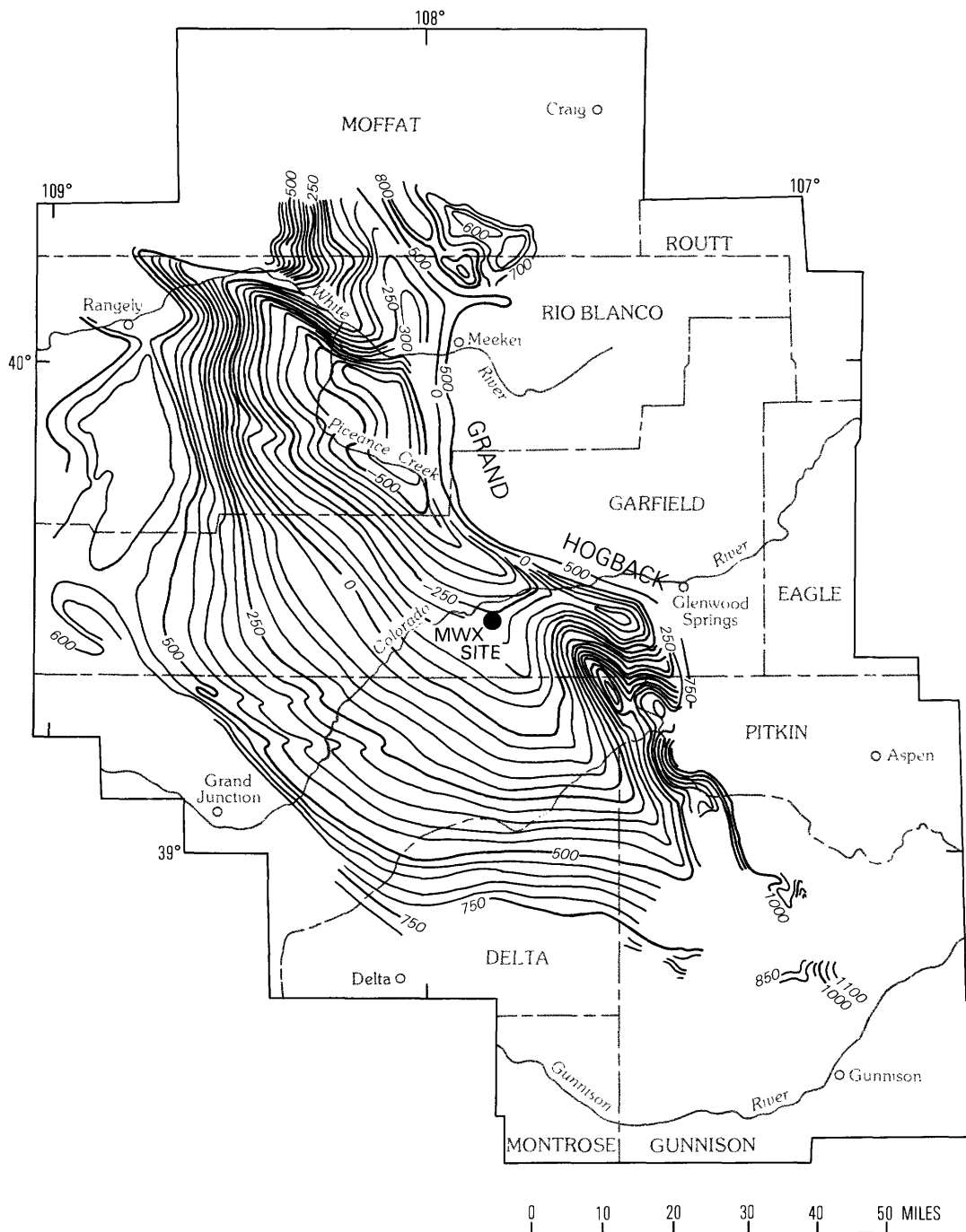


Figure 2. Structure-contour map of top of Rollins Sandstone Member of Mount Garfield Formation and equivalent Trout Creek Member of Iles Formation, Mesaverde Group, Piceance basin, Colorado. Contour interval variable; contour values in tens of feet. Modified from Johnson (1988).

basin (fig. 2). This project, referred to as the Multiwell Experiment (MWX), was undertaken as a major part of DOE's Fossil Energy Western Gas Sands Subprogram in order to provide new and improved technology to identify natural gas in tight reservoirs and to develop economically viable and reliable recovery methods (Northrop and others, 1984; Spencer, 1984). Three

closely spaced wells, designated CER Nos. 1, 2, and 3 MWX (referred to as MWX-1, -2, and -3, respectively, in this study), were drilled and logged at the MWX site to evaluate well-interference production testing in tight sandstones common to all three wells. Figure 3 shows the locations of the three wells relative to each other at the surface and at various subsurface depths. The wells, in

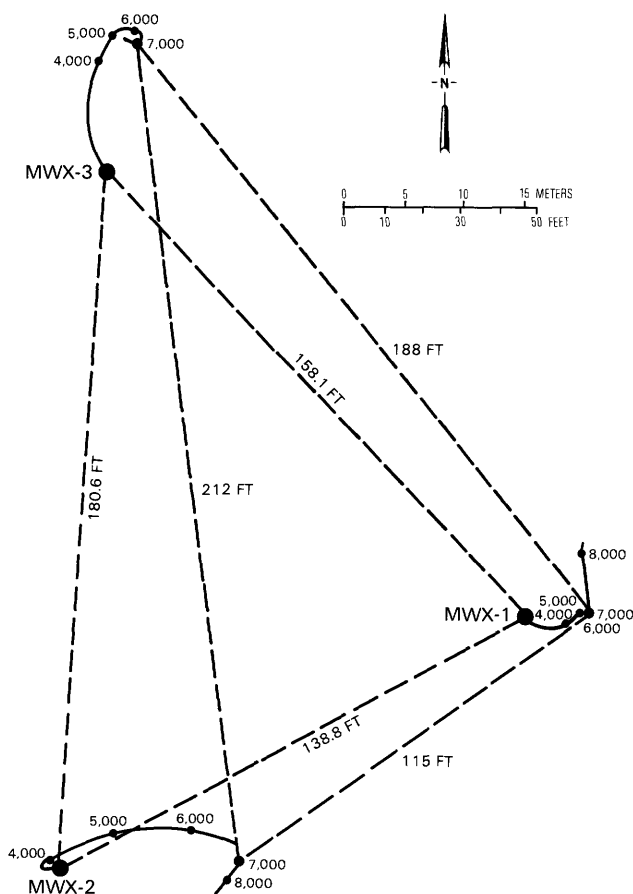


Figure 3. Relative positions of MWX wells. Large circle, surface location of well; small circle, subsurface location of well and depth (in feet). Modified from Mann (1984).

the northwest quarter of sec. 34, T. 6 S., R. 94 W., Garfield County (fig. 1), were spudded in the upper part of the lower Tertiary Wasatch Formation and reached total depth at or near the base of the Upper Cretaceous Mesaverde Group.

Approximately 4,000 ft (1,220 m) of core, extending from depths of 4,170 to 8,141 ft (1,271–2,481.4 m), was cut in various intervals in the Mesaverde with nearly complete recovery (fig. 4). The primary focus of our study was the fluvial part of the Mesaverde Group because, in this unit, low-permeability gas-bearing reservoir sandstones are complexly interbedded with discontinuous source rocks. In other Rocky Mountain basins, similar rock sequences commonly are more than 5,000 ft (1,524 m) thick. The cores taken in each well were used to characterize lateral and vertical variations in sandstone geometry; determine factors governing reservoir quality; document the character and distribution of natural fractures in blanket (marine and marginal-marine) and lenticular (nonmarine) reservoir sandstones; and apply the knowledge gained in our analysis to gas-recovery technology. Historically,

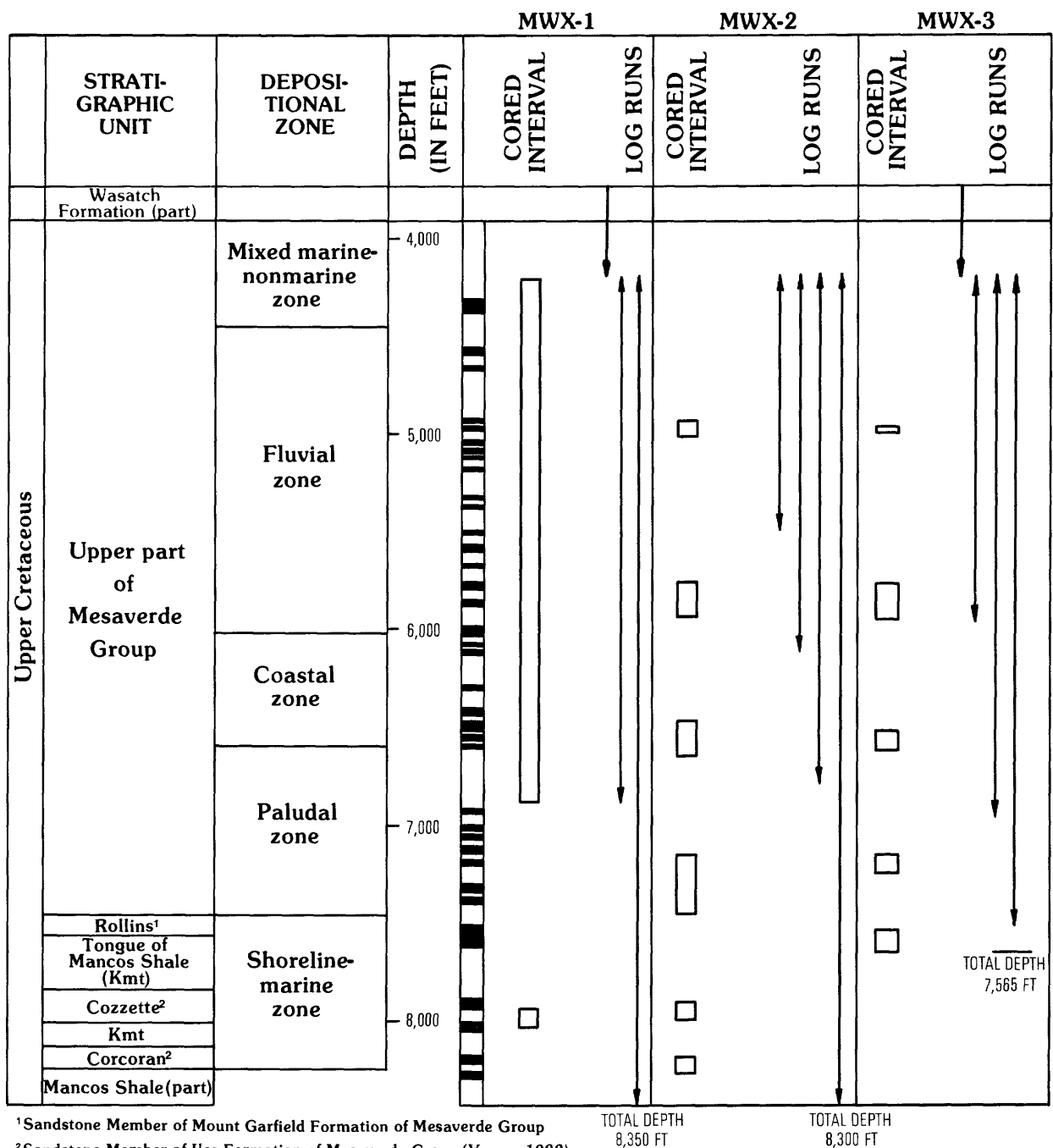
hydraulic fracturing has been relatively unsuccessful in stimulating gas production in low-permeability lenticular Cretaceous rocks, although it has been somewhat more successful in blanket reservoir sandstones of similar age (Spencer, 1985).

The goal of our study was to summarize the mineralogy and diagenesis of cored sandstones in various depositional zones in the MWX wells in order to determine the factors controlling reservoir quality and distribution, with special emphasis on individual sandstones that have been tested for gas potential. We also evaluated reservoir properties by utilizing information derived from geophysical logs. Kukal and others (1983) have described some log-analysis problems and possible solutions to these problems (Kukal, 1984). We investigated the clay mineralogy of discrete sandstone-shale pairs in an attempt to explain the effect of shale clay-mineral assemblages on the composition and abundance of clays in nearby reservoir sandstones. Collectively, our efforts should provide a better understanding of the exploration and production of hydrocarbons from tight sandstone reservoirs in the east-central Piceance basin and in other areas where rocks with similar characteristics have undergone comparable depositional and diagenetic histories.

Acknowledgments.—We acknowledge the financial and technical support of the U.S. Department of Energy (DOE). The work on which this report is based was funded by the DOE Morgantown Energy Technology Center (METC). We gratefully acknowledge the advice and encouragement of Karl-Heinz Frohne and Charles A. Komar (METC), and James Chism and J. Keith Westhusing (DOE Bartlesville Project Office). We also acknowledge the technical help of U.S. Geological Survey personnel Larry Warner, Virginia Hill, Carl Martinez, and Mark Lickus. Debra Higley did the computer processing to retrieve mineralogic point-count data provided by Bendix Field Laboratory. Most of the thin sections and the mineralogic data were provided by Bendix Field Laboratory. We also thank the personnel of Sandia National Laboratories and CER Corporation for providing support data and samples used in this study.

ANALYTICAL METHODS

Representative sandstone samples from the MWX wells were split into three portions for thin-section, X-ray diffraction (XRD), and scanning electron microscopic (SEM) analyses. For comparative purposes, a selected group of sandstone-shale pairs was analyzed by using XRD for whole-rock chemical composition and clay mineralogy. Thin sections prepared by vacuum impregnation of low-viscosity blue epoxy were stained for feldspar and calcite using standard techniques. The



¹Sandstone Member of Mount Garfield Formation of Mesaverde Group

²Sandstone Member of Iles Formation of Mesaverde Group (Young, 1982)

Figure 4. Depositional zones, discrete sandstone beds (in black), cored intervals, and individual log runs in MWX wells. Modified from Sattler (1984, fig. 1); depositional zones adapted from Lorenz (1983).

petrographic descriptions and interpretations presented in this study are based on point-count data provided by Bendix Field Laboratory (written commun., 1984). Qualitative and semiquantitative XRD analysis was performed on selected whole-rock samples and their <2 μm fractions. (Details of the XRD methods are reported by Pollastro, 1984.) Small, freshly fractured chips of sandstone were studied by using the scanning electron microscope to document the occurrence and distribution

of authigenic mineral cements and clay constituents and to characterize the morphology of pores.

PETROLOGY AND MINERALOGY

The Mesaverde Group in the southern Piceance basin was subdivided by Lorenz (1983) into five zones, paralic, fluvial, coastal, paludal, and shoreline-marine, based on the sedimentologic and depositional regime in

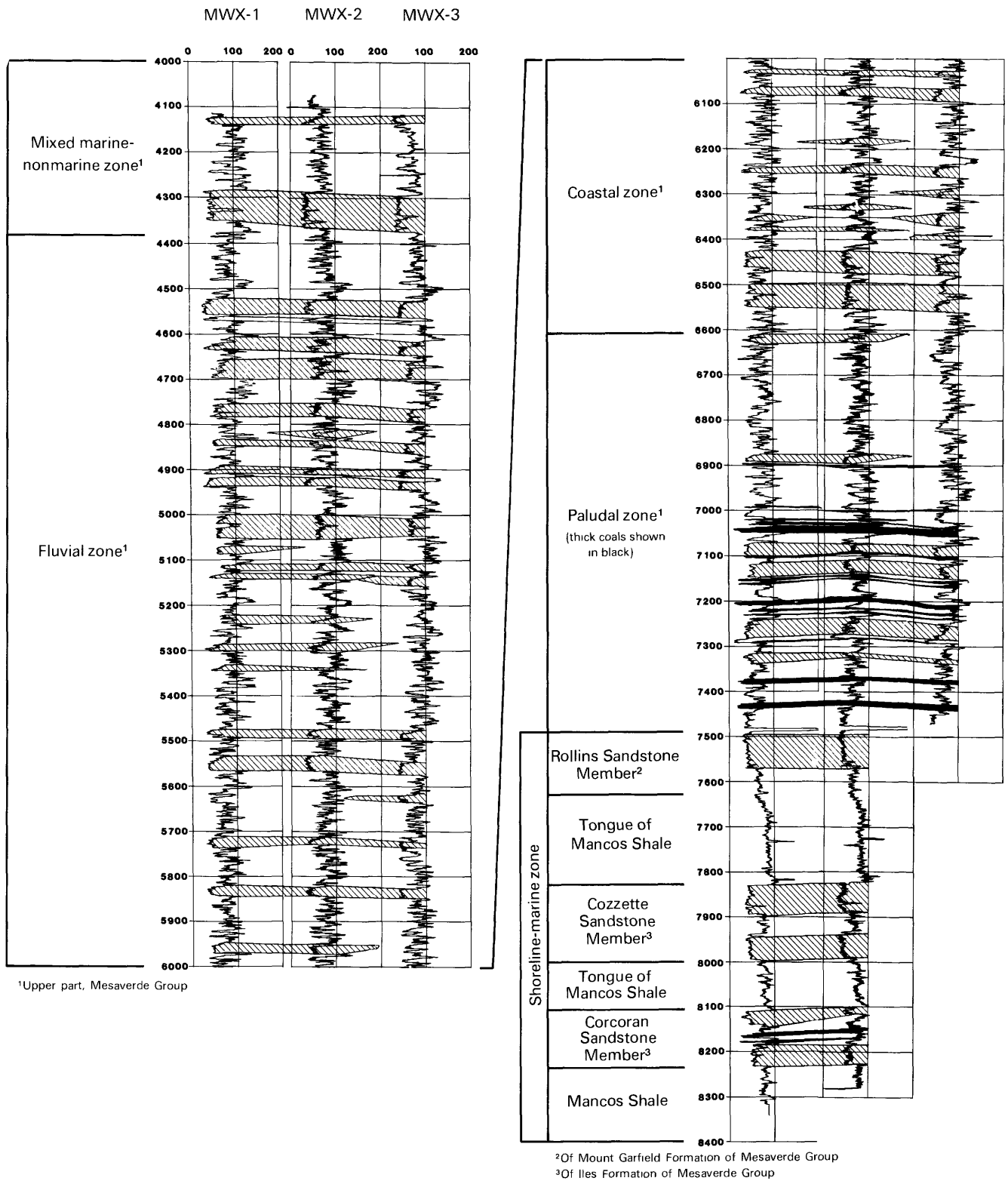


Figure 5. Gamma-ray log profiles through MWX wells showing lateral continuity of discrete sandstone units (pattern). Depth in feet also shown. Modified from Northrop (1985).

Table 1. Mineralogy of sandstones in MWX wells as calculated by using X-ray diffraction

[In weight percent. A, average; R, range. Thirty-eight core samples analyzed from each depositional zone)]

| Environment | Quartz | | Feldspar | | Carbonate minerals | | Clays (phyllosilicates) | |
|------------------------|--------|-------|----------|------|--------------------|------|-------------------------|-------|
| | A | R | A | R | A | R | A | R |
| Mixed marine-nonmarine | 62 | 53-66 | 4 | 2-5 | 15 | 9-28 | 19 | 17-20 |
| Fluvial | 51 | 33-65 | 10 | 4-21 | 8 | 1-40 | 26 | 19-36 |
| Coastal | 53 | 50-65 | 7 | 5-29 | 9 | 4-19 | 27 | 18-34 |
| Paludal | 46 | 29-55 | 6 | 4-8 | 20 | 9-43 | 29 | 24-38 |
| Shoreline-marine | 65 | 64-66 | 7 | 5-8 | 5 | 3-7 | 24 | 19-28 |

which they formed. Lorenz's paralic zone is hereafter referred to as the mixed marine-nonmarine zone. Figure 5 shows these zones and the continuity of individual sandstone beds between the three wells. Sandstones in the Mesaverde are composed dominantly of framework quartz, feldspar and lithic fragments, authigenic carbonate minerals including calcite, dolomite, and ankerite, and clay minerals including illite, mixed-layer illite/smectite (I/S), kaolinite, and chlorite. The relative distribution of these minerals within and between individual zones is shown on plate 1. The mineralogy of sandstones and shales in each of the zones was calculated by using XRD analysis (table 1).

Mineralogic data (table 1) show that, on average, rocks of the mixed marine-nonmarine and shoreline-marine zones contain the most quartz; however, the variation in amount of quartz is relatively narrow, particularly in the marine zone. The mixed marine-nonmarine and paludal zones contain more carbonate minerals than do the other zones. Clay and feldspar contents are similar in all zones except the mixed marine-nonmarine, which contains smaller amounts of these minerals. Volcanic grains are absent in the paludal and shoreline-marine zones.

Mixed Marine-Nonmarine Zone

Rocks in the mixed marine-nonmarine zone in the MWX well extend from the top of the Mesaverde Group at a depth of 3,901 ft to about 4,390 ft (1,189–1,338 m) and unconformably underlie the Tertiary Wasatch Formation. The mixed marine-nonmarine zone has been interpreted by Lorenz (1982) to represent sedimentation associated with a marine transgression correlative with the Upper Cretaceous Lewis Shale. Rocks comprising this zone were deposited in a mixed marine-nonmarine

environment and are composed dominantly of laterally continuous, hummocky, cross-stratified sandstones that contain marine fossils (Lorenz, 1982). The sandstones are composed of angular to subrounded quartz grains, sodium and potassium feldspars, and sedimentary lithic fragments. Based on the proportions of these constituents, the sandstones are classified as litharenites and feldspathic litharenites (fig. 6). Textural relations between detrital grains, authigenic minerals, and pores are shown in figure 7. Semiquantitative XRD analysis indicates that sandstones from the mixed marine-nonmarine zone contain 17–20 weight percent total clay (table 1). Much of this clay, which includes all micaceous minerals, can be attributed to altered sedimentary rock fragments of dominantly siltstone, mudstone, and shale.

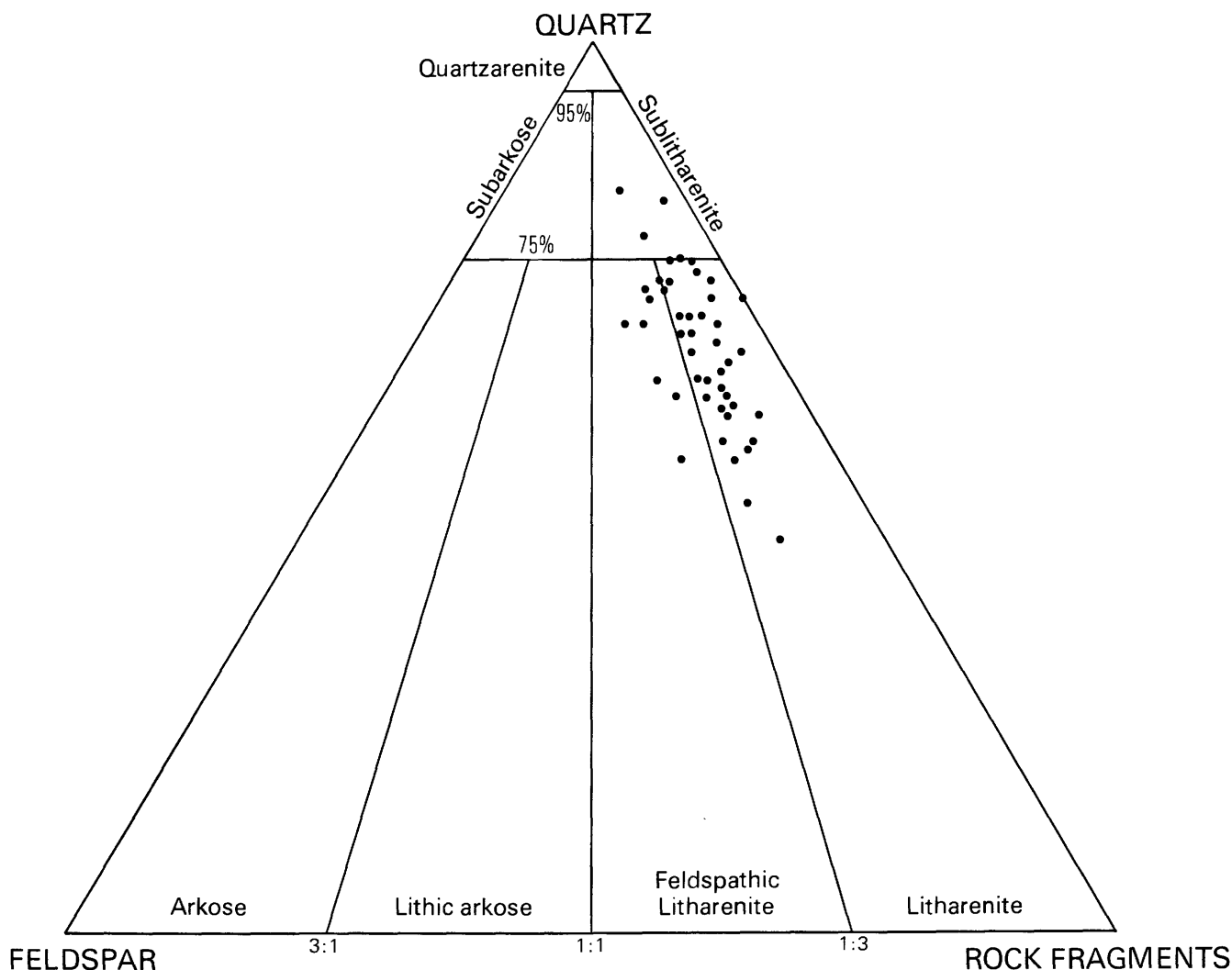
Framework Grains

Quartz, a dominant framework constituent, constitutes 27–63 percent of the bulk rock. Although most quartz grains are subangular to subrounded and fine in size, a significant number are medium grained. Individual grains typically are monocrystalline, have straight to undulatory extinction, and are free of inclusions. Overgrowths are rare, probably because of the large amount of pseudomatrix.

Sodium and potassium feldspars constitute from a trace to 9 percent and from a trace to 5 percent, respectively. These petrographic data are similar to the total feldspar calculated by using XRD (2–5 weight percent; table 1). Plagioclase grains are both twinned and untwinned and either fresh or altered in appearance. Potassium feldspar grains typically show signs of chemical alteration, usually replacement by carbonate along cleavage traces. Later dissolution of this carbonate during diagenesis results in preservation of only relict feldspar. Internal voids in feldspar grains that do not contain carbonate remnants may be the result of direct dissolution rather than carbonate removal.

Sedimentary rock fragments are abundant and constitute 5–26 percent of the rock. Mudstone, siltstone, and clay-rich shale fragments typically have been deformed between framework grains to form a pseudomatrix. These grains may be partly dissolved. A few rounded grains of detrital polycrystalline dolomite also were observed.

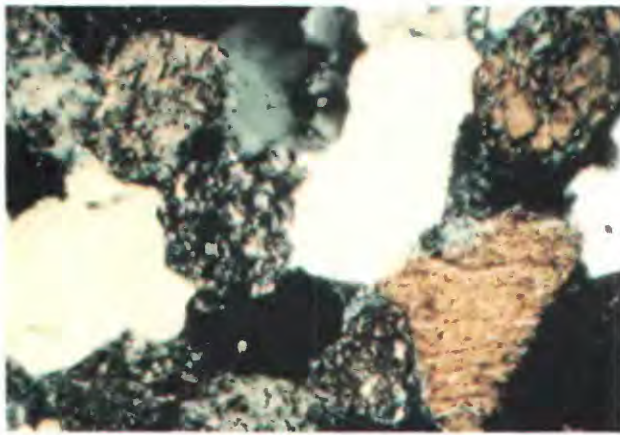
Subrounded grains of chert are abundant and make up 1–12 percent of the whole rock. Most chert is composed either of cryptocrystalline quartz crystals or of individual grains of quartz of various sizes. Grains of altered chert are various shades of brown, and in plane-transmitted light may contain inclusions of mica or black flecks of organic material. A few chert grains are black and contain veins of quartz. Some felsite grains composed of tiny quartz or feldspar crystals were likely misidentified as chert.



Authigenic Minerals

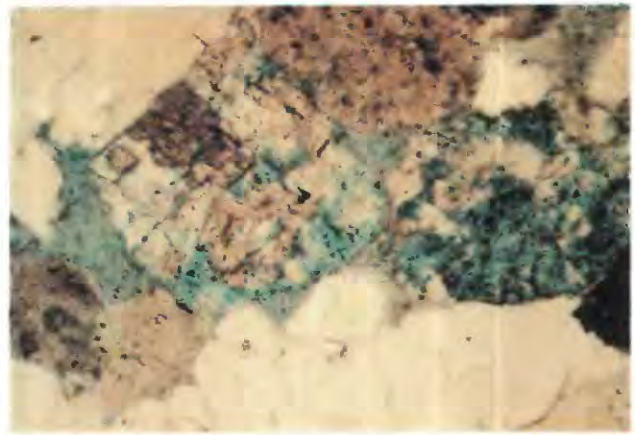
Authigenic calcite constitutes 1–42 percent of the rock in the mixed marine-nonmarine zone and is locally widespread between 4,197 and 4,271 ft (1,279–1,302 m);

Authigenic dolomite is present in trace amounts, and its occurrence is similar to calcite in that it is an anhedral pore-fill cement and replacement mineral. Some calcite locally has been dolomitized.



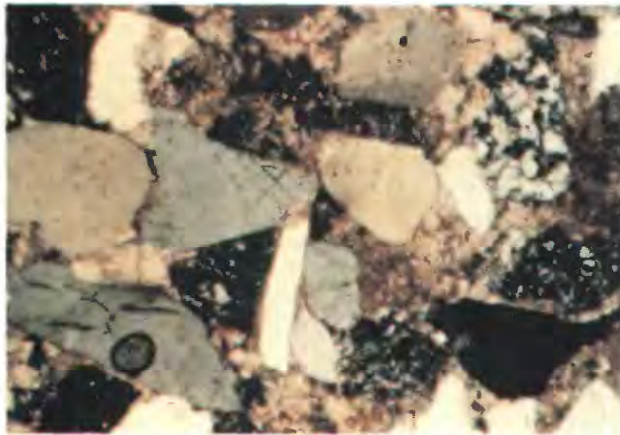
A

0.1 mm



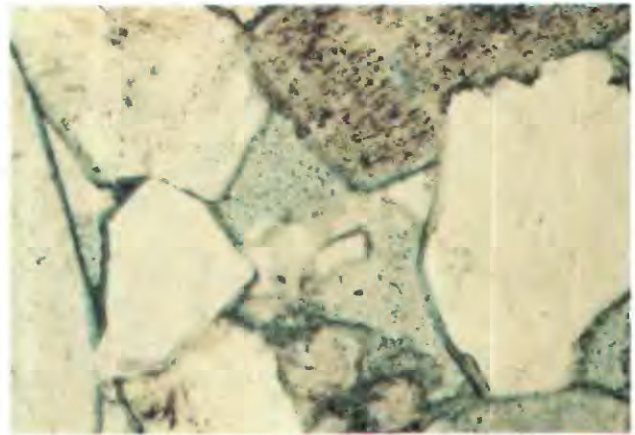
B

0.1 mm



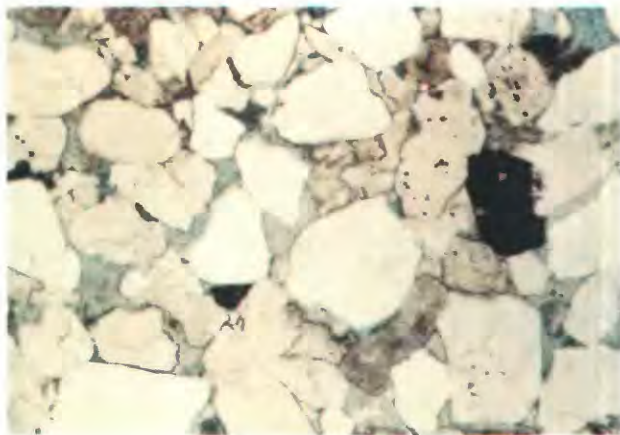
C

0.1 mm



D

0.1 mm



E

0.1 mm

Authigenic illite, iron chlorite, kaolinite, and I/S are abundant in secondary pores. Iron chlorite occurs as pseudo-hexagonal platelets oriented perpendicular to detrital grain surfaces. In rocks where iron chlorite is abundant, it coats detrital framework grains and lines

Figure 7. Thin-section photomicrographs showing detrital constituents, mineral cements, and dissolution features in sandstones of mixed marine-nonmarine zone, MWX wells. *A*, Framework grains comprising quartz (white), feldspar (yellow), and chert (dark gray). *B*, Partly dissolved feldspar grains (probably plagioclase); blue indicates porosity. Feldspar grain slightly left of center partly replaced by carbonate. *C*, Authigenic pore-fill and replacement carbonate (beige). *D*, Early iron chlorite (green) lining pores and coating framework grains; intergranular pores occluded by kaolinite. *E*, Preserved primary porosity and minor mechanical compaction reflect early iron chlorite that coated framework grains.

pores. The relatively good secondary porosity of sandstones in the mixed marine-nonmarine zone can be attributed to early formation of iron chlorite, which prevented early quartz cementation.

Authigenic kaolinite is distributed as well-crystallized booklets in dissolution voids that commonly are lined with iron chlorite. In some areas, kaolinite

completely occludes pores; in other areas, it replaces feldspar grains. Most kaolinite is interpreted to have formed during late diagenesis after carbonate dissolution.

Reservoir Properties

Porosity in the mixed marine-nonmarine zone is highly variable (0.7–9.7 percent). Most porosity is of secondary origin and results from the dissolution of chemically unstable framework grains and pore-filling and replacement carbonate cements. Core samples having the highest porosity reflect small amounts of mechanically unstable grains and detrital matrix, the formation of early iron chlorite and calcite that prevented significant quartz overgrowths, and the dissolution of carbonate cement during late-stage diagenesis. Low-porosity sandstones contain either abundant authigenic kaolinite in isolated secondary pores or widespread carbonate grains and cement that have undergone little or no dissolution.

Conventionally measured core permeability in the mixed marine-nonmarine zone varies from less than 0.01 to 1.0 mD. If permeability values were corrected for in situ stress, water saturation and gas slippage, the average permeability probably would be less than 0.01 mD. Permeability in these sandstones is partly a function of the proportion of authigenic clay. In sandstones having a well-developed open pore system and containing minor amounts of clay, permeability is more than 0.01 mD. Dry core permeability, however, is more typically 0.1 mD or less and reflects a complex micropore network that is generally disconnected as a result of extensive authigenic clay mineral development and intergrain penetration.

Borehole-geophysical logs indicate that sandstones in the mixed marine-nonmarine zone commonly have high apparent-water saturations (S_w 60–100 percent). Some of these log responses may result, in part, from clay coats on mineral grains that tend to reduce formation resistivity, or they may indicate water-bearing sandstones. Variable amounts of calcite and dolomite are reflected in a wide range of grain densities (2.61–2.71 g/cm³) that typically cause erroneous log porosity calculations.

Fluvial Zone

Analysis of borehole geophysical logs indicates that several sandstone units in the fluvial zone (4,390–6,000 ft; 1,338–1,829 m) are potential gas reservoirs and good targets for testing. The lower part of the fluvial interval (5,000–6,000 ft; 1,524–1,829 m) is of considerable interest for its gas potential because numerous sandstones contain interconnected, partly open, vertical

fractures that greatly enhance effective permeability to gas in otherwise very low permeability rocks.

The fluvial zone dominantly comprises lenticular, crossbedded, channel-form sandstones and rare carbonaceous shales, mudstones, and siltstones. Both the bed-form geometry and upward-fining trend in grain size indicate sediment deposition in a fluvial environment (Lorenz, 1982, 1983). The mineralogic composition of individual sandstone units varies locally, but, using normalized proportions of quartz, feldspar, and lithic fragments, most of the sandstones are lithic arkoses and feldspathic litharenites (fig. 8). Thin-section photomicrographs (fig. 9) show relationships between the detrital grains and authigenic mineral cements.

Framework Grains

Quartz is the dominant framework constituent in the fluvial sandstones (10–64 percent). It comprises single, subrounded to subangular, monocrystalline grains that generally are free of inclusions. In the interval from 5,820 to 5,840 ft (1,774–1,780 m), quartz grains have a bimodal size distribution. Sandstones in the interval from 5,000 to 5,050 ft (1,524–1,539 m) are unusual in that they contain a large number of quartz grains that display undulatory rather than straight extinction; undulatory extinction indicates stress deformation due to compaction. Overgrowths on framework quartz grains typically are rare because of the large amounts of pseudomatrix that fill pores. In sandstones containing no lithic fragments, quartz grains commonly are interpenetrating and syntaxial overgrowths occur locally. Most grain boundaries are long to concave-convex, but boundaries are sutured in areas of extensive grain compaction.

Sodium and potassium feldspar compose 2–26 volume percent and from a trace to 21 percent, respectively. Feldspar is most abundant in the interval from about 4,970 to 5,160 ft (1,515–1,573 m). Plagioclase feldspar is common to all samples (5–15 weight percent by XRD), whereas potassium feldspar is only in samples containing more than 10 weight percent plagioclase and may constitute as much as 10 weight percent of the bulk rock. Feldspar occurs as irregular, angular, fresh to poorly preserved fragments. Relatively fresh feldspar grains often are twinned; altered feldspar grains usually are altered to clay or show signs of incipient sericitization. Many potassium feldspar grains have been partly to completely dissolved and display a skeletal texture, probably as the result of earlier replacement by carbonate and subsequent dissolution. In some sandstones, partly leached feldspar grains appear to have been dissolved in situ by interstitial pore fluids because relicts of early carbonate cement are not associated with the existing grains. Moldic pores probably result from the removal of feldspar by dissolution processes.

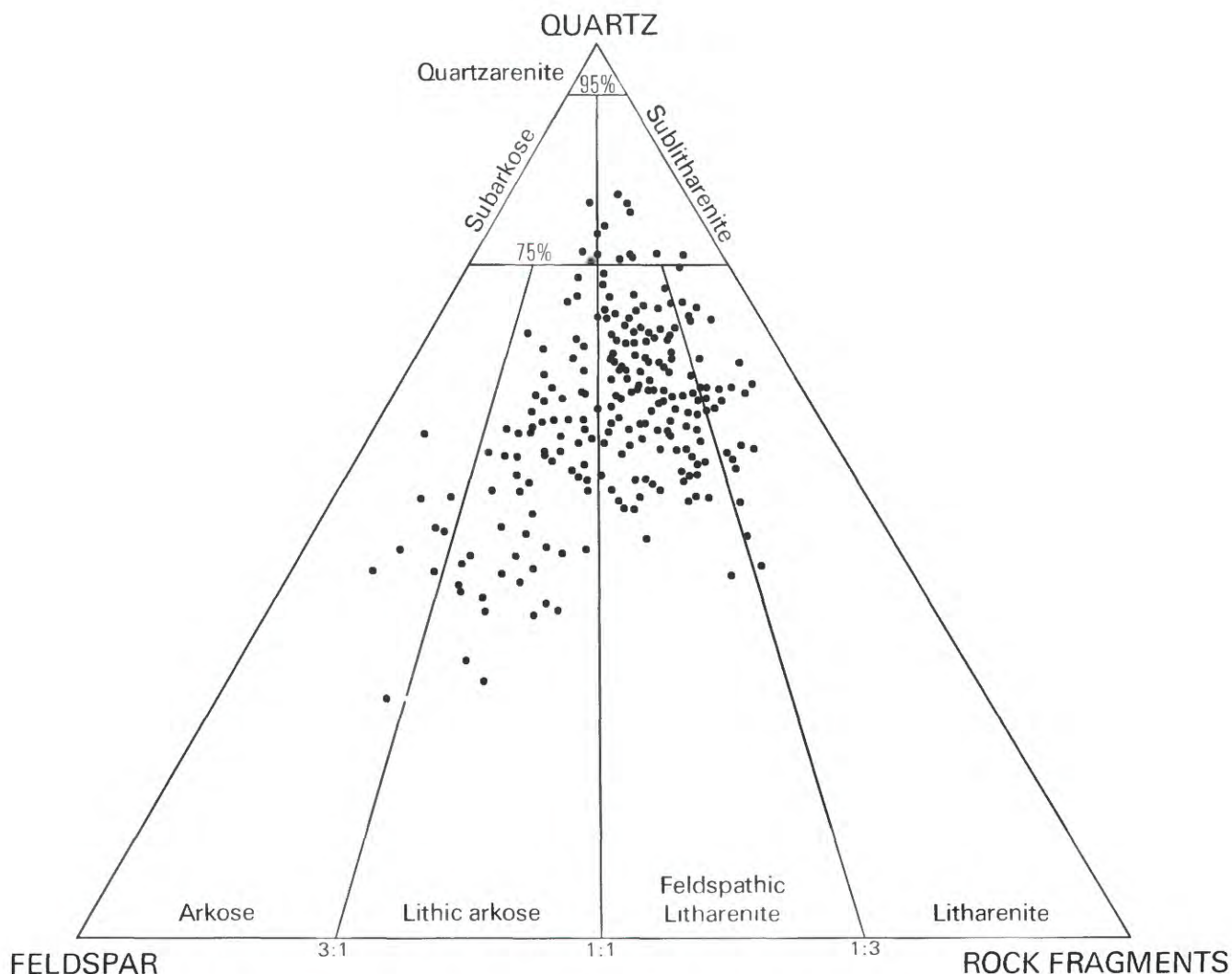


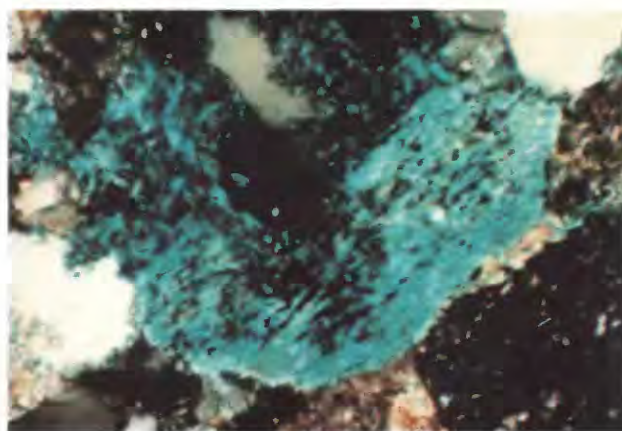
Figure 8. Mineralogic compositions of framework grains in sandstones of fluvial zone, MWX wells. Diagram modified from Folk (1974).

Most lithic fragments in sandstones of the fluvial zone are sedimentary and volcanic in origin. The most abundant lithic variety is chert, which constitutes from a trace to 13 percent of the rock. Much of the chert is composed of interlocking quartz crystals that vary from cryptocrystalline to polycrystalline in size. Many grains identified as chert are composed of large discrete crystals of quartz in a cryptocrystalline groundmass. Although some chert grains are clear and unaltered, most are altered and vary from light to dark brown. Unaltered chert grains often do not contain mineral inclusions, whereas altered chert grains display tiny flakes of mica, inclusions of carbonaceous material, and small crystals of dolomite. A few chert grains are almost black and may contain veins of quartz or chalcedony.

Other lithic fragments that occur locally include varying amounts of mudstone, clay-rich shale, siltstone, detrital carbonate (principally dolomite), and minor

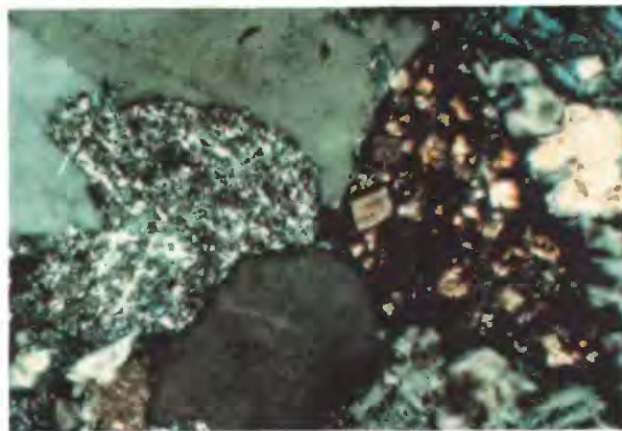
metamorphic grains. Many of these lithic fragments cause the sandstones to appear “shaly” on borehole-geophysical logs. Mudstone, shale, and siltstone are commonly extensively sericitized and are difficult to identify because they form a pseudomatrix between framework grains. This pseudomatrix was not included in the point-count data (pl. 1). Extensive deformation of these mechanically and chemically unstable grains during early diagenesis eliminated much of the original porosity in the sandstones.

Detrital carbonate fragments are abundant in many of the sandstones and distributed as medium-brown, partly abraded elliptical clasts and as twinned, subangular rhombohedral fragments. The cleavage fragments commonly contain a dark-brown outer rim that is enriched in iron relative to the inner core. Both types of detrital carbonate are similar in size to adjacent framework grains.



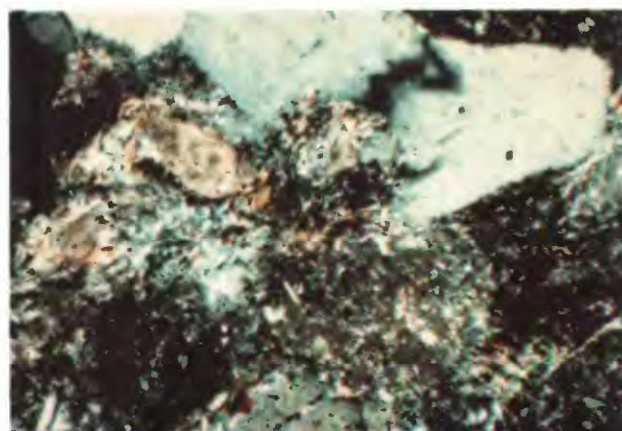
A

0.1 mm



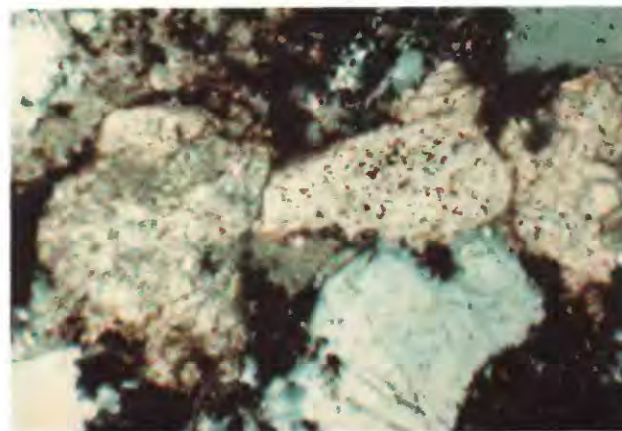
B

0.1 mm



C

0.1 mm



D

0.1 mm

Figure 9 (above and facing page). Thin-section photomicrographs showing framework grains, authigenic cements, porosity, and mineralized fractures in sandstones of fluvial zone, MWX wells. *A*, Partly dissolved plagioclase grain; blue indicates intergranular porosity. *B*, Two varieties of chert; grain on right side of the photograph contains rhombic inclusions of dolomite. *C*, Sericitized sedimentary lithic fragments. *D*, Rounded and abraded detrital dolomite grains. *E*, Volcanic rock fragment containing laths of plagioclase feldspar in fine-grained groundmass. *F*, Authigenic syntaxial quartz overgrowths that formed during early diagenesis. *G*, Early pore-fill and replacement calcite (beige). *H*, Secondary porosity (blue), probably resulting from carbonate dissolution. *I*, Bifurcating fracture cemented with calcite.

Lithic fragments present in minor amounts include stretched polycrystalline quartz grains (quartzite) composed of interlocking quartz crystals that have strongly sutured grain boundaries. Grains of volcanic origin contain blocky to equant laths of feldspar in an altered fine-grained groundmass. Most volcanic grains are in the interval from 5,000 to 5,050 ft (1,524–1,539 m); some felsite grains composed of fine-crystalline quartz or feldspar may have been misidentified as chert.

Authigenic Minerals

Authigenic minerals in the fluvial sandstones include minor secondary quartz, varying amounts of

carbonate minerals (principally calcite and dolomite), and the clay minerals illite, mixed-layer I/S, iron-rich chlorite, and kaolinite.

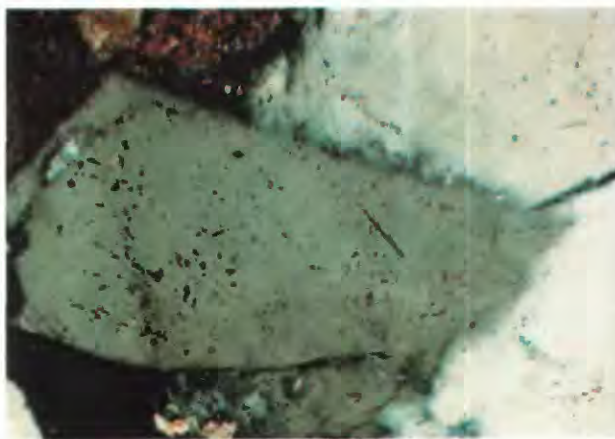
In areas containing only small amounts of deformed framework grains and detrital matrix, secondary quartz is present locally. In these areas, authigenic quartz overgrowths coalesce.

Authigenic carbonate minerals generally are poorly developed but in some fluvial sandstones are locally widespread (as much as 48 percent). Calcite is the most common variety of authigenic carbonate (0–48 percent) and occurs as a poikilotopic pore-filling cement and a grain replacement. In areas where calcite is



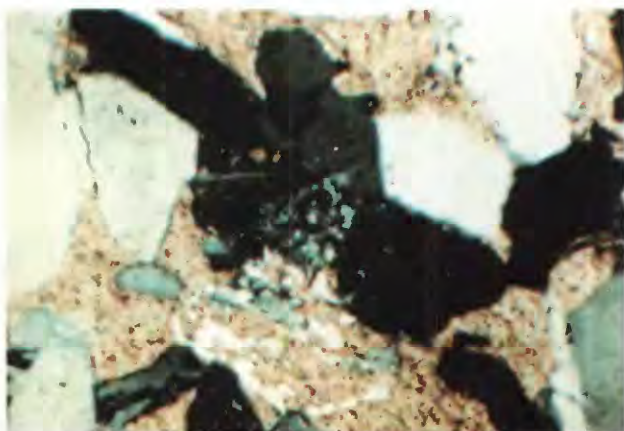
E

0.1 mm



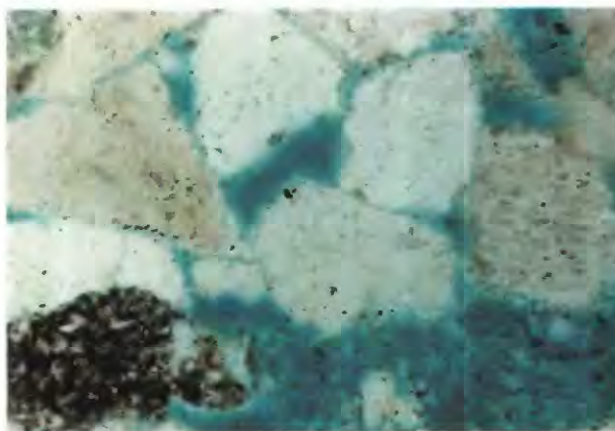
F

0.1 mm



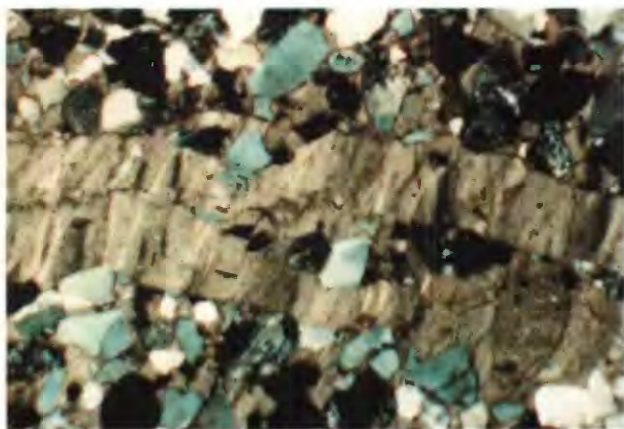
G

0.1 mm



H

0.1 mm



I

0.2 mm

extensively developed, it encloses angular and relatively unaltered framework grains. Its early diagenetic formation probably prevented further alteration by pore fluids. In many sandstones, relicts of calcite in inter- and intragranular pores suggest that preexisting calcite was

widespread in sandstones now containing abundant secondary porosity. Partly dissolved framework grains (particularly feldspar) and corroded overgrowths and grain boundaries provide additional evidence for early calcite cement.

In the interval from 5,000 to 6,000 ft (1,524–1,829 m), authigenic calcite commonly fills fractures (fig. 9I). Both the origin and distribution of fracture-fill minerals in Mesaverde Group rocks have been discussed by Pitman and Sprunt (1986).

Authigenic dolomite is present in variable amounts (0–33 percent) and occurs as an anhedral pore-fill and replacement mineral. In many sandstones, it is most abundant wherever detrital dolomite grains may have served as nuclei for its growth. Although authigenic dolomite may be iron bearing, the sandstone samples were not specifically stained for iron carbonate.

Authigenic clay is abundant in dissolution voids. Illite and I/S typically are fibrous and form a thin coating on framework grains and fill residual pores. Kaolinite occurs as well-crystallized pseudohexagonal booklets that occlude secondary pores commonly lined with illite or chlorite, and it has partially replaced some unstable framework grains such as feldspar. Textural relations indicate that kaolinite precipitated late, and probably last.

In some sandstones of the fluvial zone, iron-bearing chlorite occurs as clay coats and pore-linings composed of individual platelets oriented perpendicular to a grain surface. (See Pollastro, 1984, for XRD identification and morphology.) Chlorite formed early because other mineral cements, such as secondary quartz and early calcite, fill pores lined with chlorite. Tight sandstones that contain well-developed chlorite typically are more porous than those without chlorite pore linings; either the chlorite coats retarded quartz overgrowths and thus preserved existing pores, or preexisting pore-fill cement such as carbonate has been dissolved.

Reservoir Properties

In the fluvial zone, sandstones that have good gas potential are in the intervals 4,892–4,937 ft (1,491–1,505 m), 5,000–5,050 ft (1,524–1,540 m), 5,535–5,565 ft (1,687–1,696 m), 5,820–5,840 ft (1,774–1,780 m), and 5,950–5,970 ft (1,814–1,820 m). Porosity in fluvial sandstones ranges from less than 1.0 to 11.1 percent. Most porosity is secondary in origin and is the result of carbonate dissolution. The relatively high porosity values are from sandstones containing a significant number of open pores that were incompletely filled with authigenic clay; the relatively low values result from either destruction of original porosity by abundant deformed lithic fragments or the extensive development of authigenic clay and carbonate cement. In sandstones containing no evidence for early carbonate development, visible porosity most likely formed by dissolution of framework feldspar.

Conventional core-measured permeability is from less than 0.1 to 1.0 mD and is best developed in

sandstones containing abundant open vertical fractures. In areas where fractures are cemented by carbonate, the carbonate may act as a barrier to fluid flow and greatly reduce permeability. If fractures are incompletely cemented, however, permeability may be higher than in the enclosing sandstone matrix.

On the basis of geophysical log response, most sandstones in the interval from 5,000 to 6,000 ft (1,524–1,829 m) are gas bearing but have relatively low porosity (typically less than 10 percent); computer-processed logs indicate that most porosities are less than 12 percent. A crossplot of core porosity and conventionally measured permeability in the MWX-2 well indicates that permeability generally increases as porosity increases (fig. 10); the correlation coefficient is 0.680 and coefficient of determination (R^2) is 0.462. A similar correlation coefficient (0.695, R^2 0.483; fig. 11) for stratigraphically equivalent rocks from the MWX-1 well indicates only a fair correlation between porosity and conventionally measured permeability in either well. Disconnected clay-filled secondary pores, characteristic of much of the existing porosity, tend to cause a poorer correlation between porosity and permeability. If a Klinkenberg correction is applied at in situ stress (Kukul and Simons, 1985), the correlation coefficient between porosity and permeability is more reasonable. Both water-saturated capillaries and pores filled with clay greatly reduce gas flow during laboratory measurements and production testing.

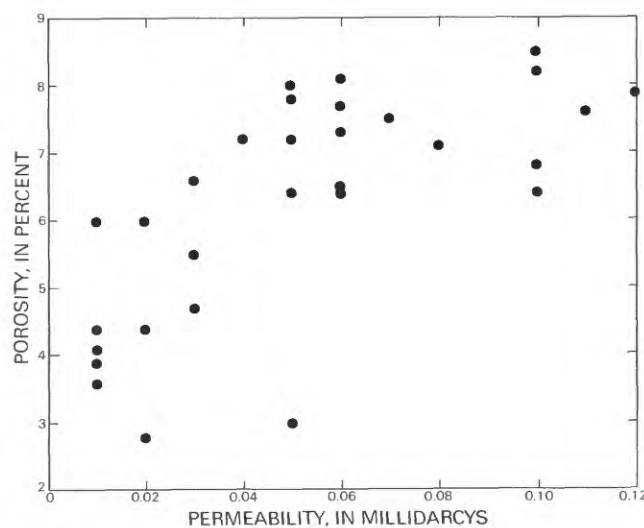


Figure 10. Core porosity and conventionally measured permeability for sandstones in interval from 5,505 to 5,855 ft (1,678–1,785 m) in fluvial zone of MWX-2 well. Permeability values <0.01 mD not included. Correlation coefficient 0.680, coefficient of determination (R^2) 0.462.

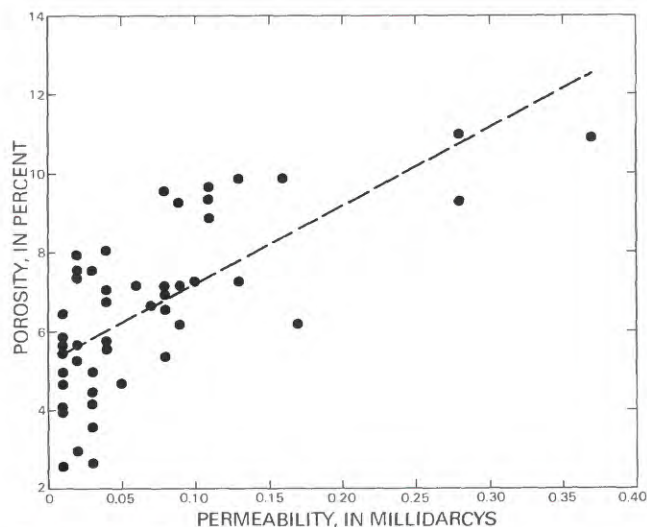


Figure 11. Core porosity and conventionally measured permeability for sandstones in interval from 5,700.5 to 5,846.3 ft (1,737.5–1,782.0 m) in fluvial zone of MWX-1 well. Correlation coefficient 0.695, coefficient of determination (R^2) 0.483. Dashed line is least-squares regression.

The deeper parts of the MWX wells are overpressured. The top of abnormally high reservoir pressures is in the lower part of the fluvial zone at about 5,600 ft (1,707 m) (Spencer, 1986, 1987). Although extensive fractures, some of which are partly open, exist from about 5,700 to 5,850 ft (1,737–1,783 m), it is uncertain if the intensity of fractures is related to overpressuring because the fracturing appears to be local. The MWX-2 and MWX-3 wells were cored at about the same depth as the fractured interval in MWX-1; however, these cores are not significantly fractured even though overpressuring was encountered at about the same depth.

Figure 12 shows a crossplot of porosity and grain density for rocks in MWX-2 stratigraphically equivalent to the fractured interval in MWX-1. The data for MWX-2 have a correlation coefficient of -0.782 and R^2 of 0.612. The apparent trends of increasing grain density and decreasing porosity are attributed to authigenic carbonate. Porosity-density data from the fractured interval in MWX-1 have a correlation coefficient of only -0.325 and R^2 of 0.105. Although the differences between MWX-1 and MWX-2 statistics are not understood, the greater abundance of natural fractures in core from MWX-1 as compared to MWX-2 suggests that microfracture porosity is concentrated in the carbonate-cemented sandstones of MWX-1.

Coastal Zone

The coastal zone extends from about 6,000 to 6,600 ft (1,829–2,012 m) and represents sediment deposition on the upper part of a deltaic plain (Lorenz, 1982, 1983).

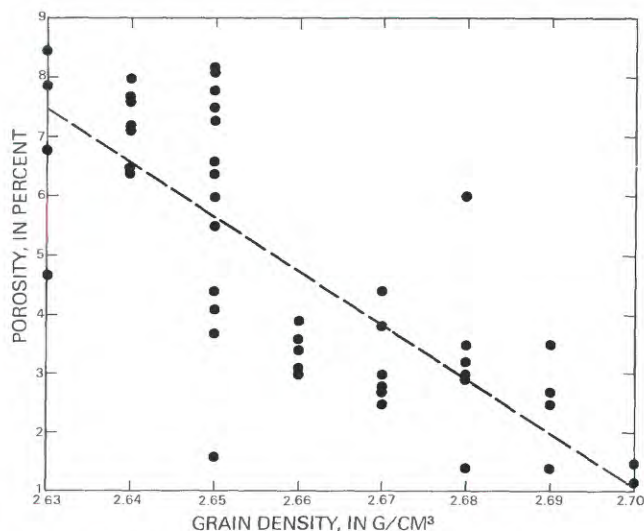


Figure 12. Core porosity and grain density for sandstones in interval from 5,705 to 5,855 ft (1,739–1,785 m) in fluvial zone of MWX-2 well. Permeability values <0.01 mD not included. Some grain densities are anomalously low and may be in error. Correlation coefficient -0.782 , coefficient of determination (R^2) 0.612. Dashed line is least-squares regression.

Sandstones in this interval generally are fine-grained, crossbedded sequences enclosed by discontinuous carbonaceous mudstones and shales, and very thin beds and lenses of coal. Coal is much less abundant in the coastal zone than in the underlying paludal and shoreline-marine zones. Sandstones in the coastal zone are mineralogically similar to sandstones in the underlying paludal zone. They are fine grained and moderately sorted, consist dominantly of quartz, lithic fragments, and minor amounts of sodium feldspar, and are classified as feldspathic litharenites (fig. 13). Figure 14 illustrates the detrital framework grains, mineral cements, and porosity in the coastal zone.

Framework Grains

Single monocrystalline quartz grains are abundant and compose from 23 to 64 percent of the rock. Most grains are subangular to subrounded, clear, and free of inclusions. Abrasion of local occurrences of overgrowths on detrital quartz grains indicate that these grains probably are reworked. Significant amounts of mechanical compaction have resulted in the interpenetration of quartz grains.

Feldspar is uncommon and composes from a trace to 9 percent by volume. It occurs as twinned angular fragments (probably plagioclase) that are commonly cloudy as a result of clay alteration.

Lithic fragments in the sandstones are predominantly of sedimentary origin and constitute 2–16 percent of the rock although volcanic grains are locally

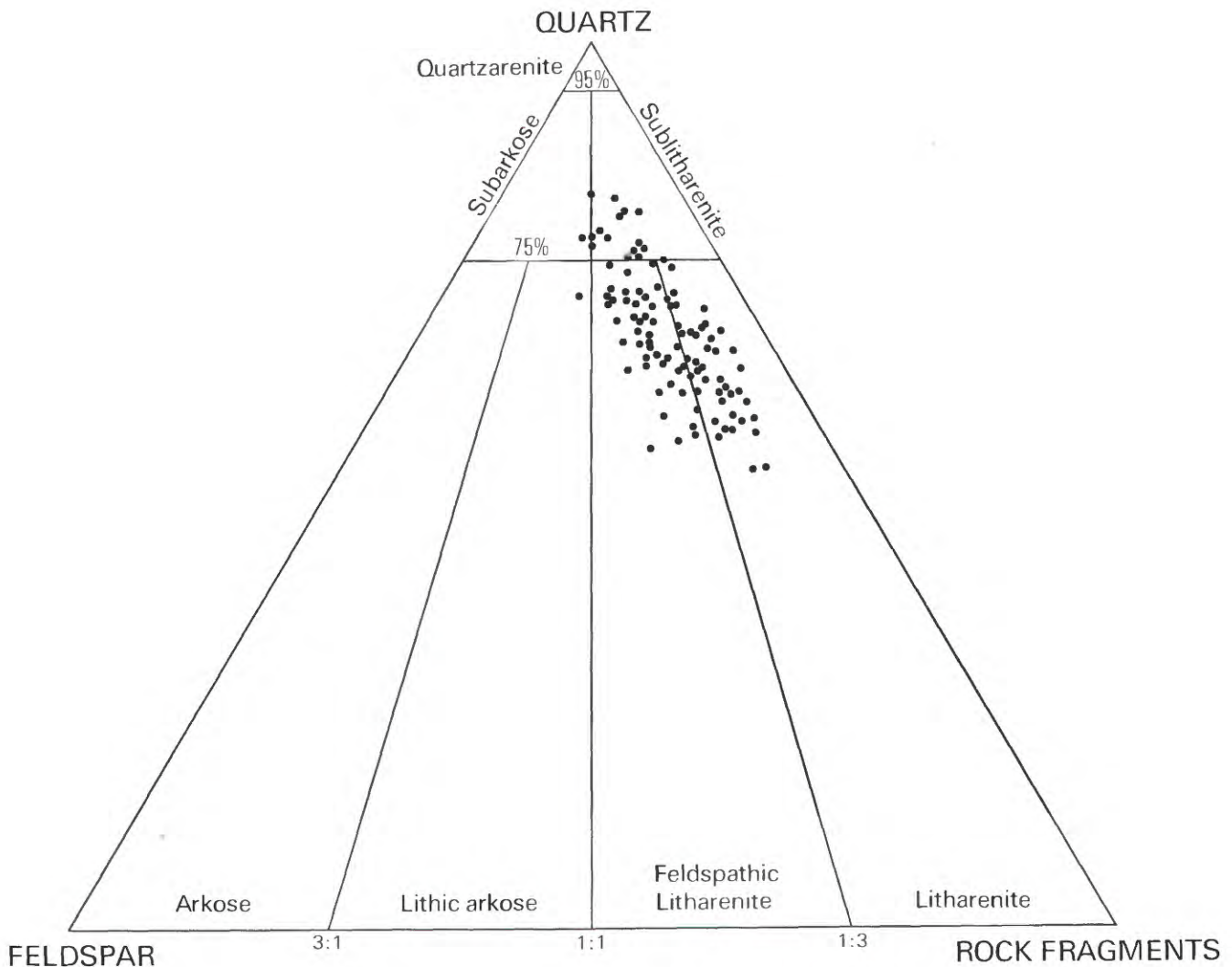


Figure 13. Mineralogic compositions of framework grains in sandstones of coastal zone, MWX wells. Diagram modified from Folk (1974).

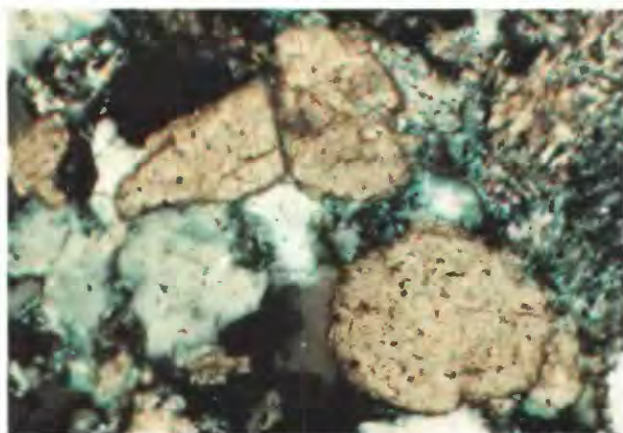
abundant. Chert is the most abundant lithic constituent and makes up 3–13 percent. Most chert grains are subangular to subrounded and typically are composed of interlocking monocrystalline quartz crystals. Some chert grains contain large discrete crystals of quartz in a microcrystalline groundmass. Although most chert grains are relatively unaltered, some are altered and are light to medium brown in plane-transmitted light. A locally abundant variety of chert is altered and contains tiny flakes of highly birefringent mica or small crystals of dolomite. A few grains of chert in many of the sandstones are dark brown to black and contain veins filled with quartz or chalcedony.

Other lithic fragments that occur locally are dolomite and calcite. Detrital carbonate clasts typically occur as elliptical polycrystalline aggregates similar or slightly larger in size than nearby framework grains. Most dolomite occurs as partly abraded, monocrystalline sub-

rhombohedral grains that have a medium-brown, euhedral to anhedral rim. Although the sandstones were not stained for iron-bearing carbonate, these characteristics suggest that these dolomite grains have an iron-free dolomite core surrounded by an iron-bearing dolomite rim interpreted as ankerite. Both the dolomite core and ankerite rim were probably transported to the present site of deposition; some of the ankerite may be an authigenic overgrowth cement.

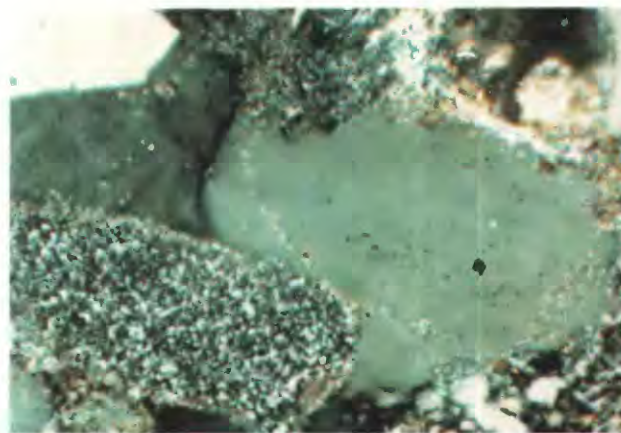
Mudstone, siltstone, and shale clasts in the sandstones commonly are difficult to recognize because they form a pseudomatrix from extensive mechanical deformation due to compaction. Many of these grains have been altered to sericite.

Volcanic grains often contain subhedral to euhedral phenocrysts of feldspar in an altered fine-grained ground mass. Some fragments of felsite are composed of either fine-crystalline quartz or feldspar.



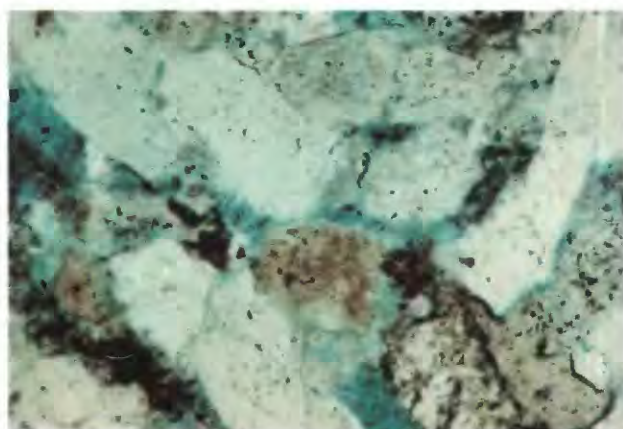
A

0.1 mm



B

0.1 mm



C

0.1 mm

Figure 14. Thin-section photomicrographs showing detrital grains, mineral cements, and porosity in sandstones of coastal zone, MWX wells. *A*, Subangular to rounded grains of detrital dolomite that have thin, dark iron-rich rims, probably ankerite. Note partly dissolved sericitized rock fragment to right of dolomite grains. *B*, Framework quartz and chert displaying thin coating of authigenic dolomite crystals that formed before secondary quartz. *C*, Porosity (blue) formed in situ by direct dissolution of matrix matter.

cement predated grain compaction and the formation of other authigenic mineral cements. Dolomite cement rims are common between interlocking quartz grains, and secondary quartz locally fills pores lined with early dolomite.

Authigenic illite and I/S are the dominant clay minerals in sandstones of the coastal zone; minor kaolinite is also present. These minerals fill and bridge primary and secondary intergranular pores and coat framework grains (fig. 15). The large surface area and fibrous habit of these clays have likely reduced porosity and permeability.

Reservoir Properties

The most favorable sandstone gas reservoirs in the coastal zone of the MWX-1 well are in the intervals 6,425–6,460 ft (1,958–1,969 m) and 6,500–6,550 ft (1,981–1,996 m). Sandstones in these intervals are thick and easily correlate with similar sandstones in the MWX-2 and MWX-3 wells. Porosity and permeability in the coastal zone typically are low (2.9–8.7 percent and <0.1–0.37 mD, respectively) and are controlled by both the compaction of mechanically unstable framework grains and matrix material and the presence or absence of carbonate cements. When tested in the laboratory, the sandstones yielded low volumes of gas, generally less than 100,000 cubic feet per day (100 MCFD), and,

Authigenic Minerals

Authigenic minerals in the sandstones include minor secondary quartz and variable amounts of calcite, dolomite, illite, and I/S. Quartz overgrowths are present locally in minor amounts and commonly have coalesced to form a cement. Secondary silica cementation predates formation of other mineral cements; however, it postdates an early stage of dolomitization.

Authigenic calcite makes up from zero to 21 percent of the rock and is distributed predominantly as isolated replacements of framework grains. In most sandstones, calcite was not widespread, and few existing pores exhibit morphological relics of preexisting carbonate. Authigenic dolomite constitutes 2–31 percent of the rock and is a pore-fill and replacement cement. Two sandstone samples (6,546.3, 6548.8 ft; 1,995.3, 1,996.1 m) show evidence for early dolomitization. In these sandstones, virtually all framework grains are coated with a thin rim of small anhedral dolomite crystals. Textural relations indicate that early dolomite

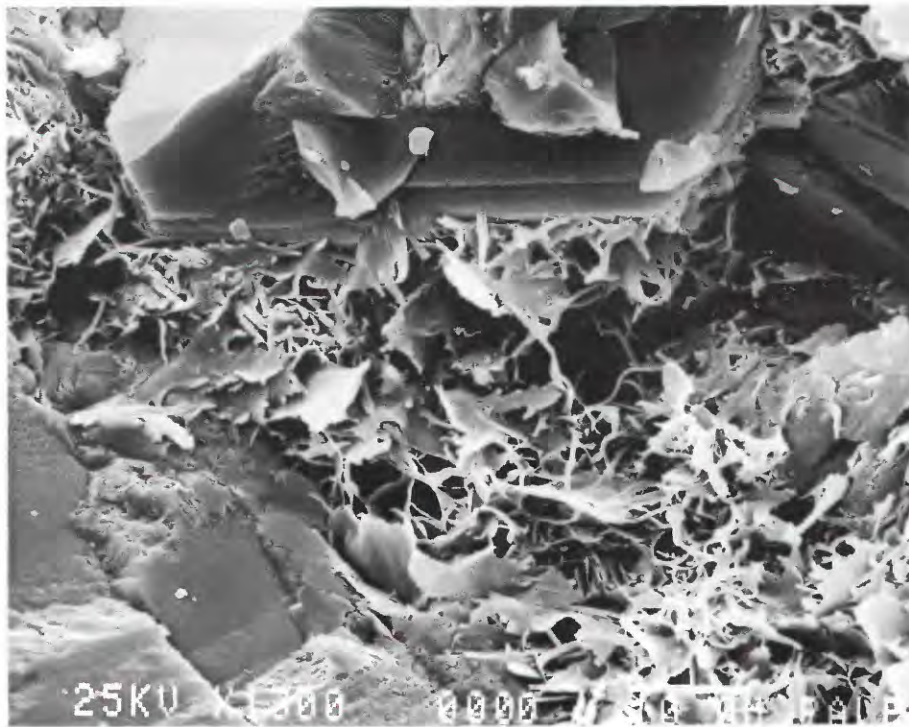


Figure 15. Scanning electron photomicrograph showing pore throat filled with bridging illite and illite/smectite. Bar scale 10 μm .

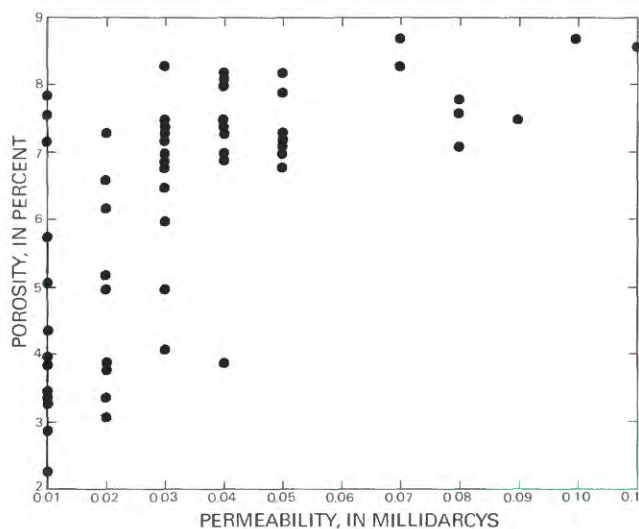


Figure 16. Core porosity and conventionally measured permeability for sandstones in coastal zone of MWX-1 well. Correlation coefficient 0.612, coefficient of determination (R^2) 0.374.

although test analysis data indicate that natural fractures were a major contributor to permeability, pressure draw-down interference was not observed in the observation wells (Paul Branagan, oral commun., 1985).

Figure 16 shows core porosity and conventionally measured permeability for sandstones in the coastal zone

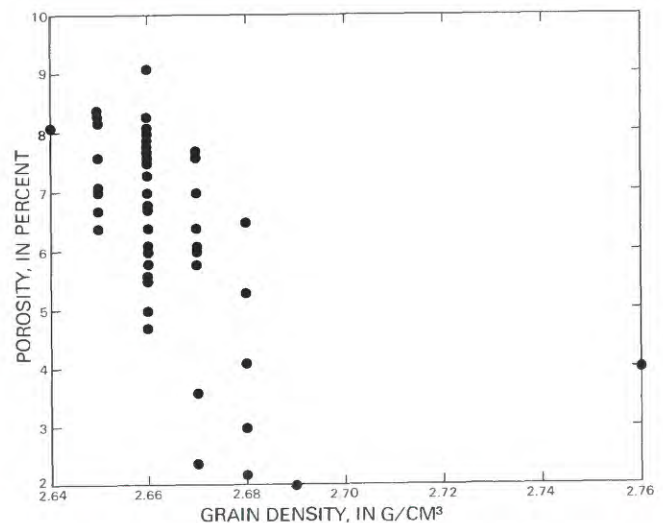


Figure 17. Core porosity and grain density of framework grains in sandstones of coastal zone of MWX-2 well.

of MWX-1 that were tested for production. The correlation coefficient of 0.612 and R^2 of 0.374 indicate a fair correlation between porosity and permeability; however, the data have not been corrected for gas slippage and confining stress. Figure 17 shows porosity and grain density for coastal-zone sandstones in MWX-2

equivalent to those tested in MWX-1. Although grain densities for most tight sandstones typically are more than 2.68 g/cm³, those from the coastal zone are somewhat lower than normal, probably because of the presence of coaly detritus. Samples having grain densities of more than 2.68 g/cm³ commonly contain detrital dolomite and carbonate cement. The general increase in grain density and corresponding decrease in porosity suggest that carbonate cement lowers porosity. Low permeabilities of the tested sandstones can also be attributed primarily to fibrous clays in pores and pore throats. At formation conditions, large amounts of water adsorbed on clay surfaces create high irreducible water saturations that result in low permeability. Fracture fluids containing potassium chloride or minimal liquids (foam) may prove effective when stimulating reservoir rocks having these characteristics.

Petrographic analysis indicates that in sandstones of the coastal zone sericite is present as an alteration product of rock fragments and mineral grains. High-spectra gamma-ray responses suggest that these rocks are shaly. Most of the response is attributed to potassium in illite and (or) sericite rather than potassium feldspar. Sericite is dielectric and causes an increase in resistivity similar to that caused by hydrocarbon saturation, whereas the cation exchange capacity of the illite and its adsorbed water content result in low resistivity. Although small amounts of illite and I/S are in pores of the coastal-zone sandstones, most of the gamma-ray response may be from coarse sericitic material. Coarse sericite crystals are not particularly detrimental to gas-flow rates, as compared to finer illite. Illite in pores decreases the percentage of gas-filled pore space because it increases water saturation.

Paludal Zone

The paludal zone extends from about 6,600 to 7,455 ft (2,012–2,272 m) and contains predominantly fine grained, crossbedded blanket and lenticular sandstones. Discontinuous carbonaceous mudstone and shale and discrete beds of coal commonly are interbedded with the sandstones. Sedimentologic studies by Lorenz (1982, 1983) indicate that these rocks represent sediment deposition in lower-delta-plain environments.

Sandstones from the paludal zone are composed of fine-grained, angular to subrounded quartz, sedimentary rock fragments (including shale rip-up clasts), and variable amounts of matrix. Feldspar is virtually absent. Normalized proportions of quartz, feldspar, and lithic fragments classify these sandstones as predominantly feldspathic litharenites (fig. 18). Textural relations between detrital grains and porosity are shown on figure 19.

Framework Grains

Detrital quartz grains are the single most abundant constituent in the sandstones and make up 17–52 percent of the rock. Most quartz grains are monocrystalline and display concave-convex contacts. Abraded overgrowths on many detrital quartz grains suggest the grains were recycled from older rocks. The absence of widespread secondary quartz in these sandstones is attributed to the presence of abundant labile grains that deformed easily during early burial and thus restricted porosity for authigenic mineral growth. Feldspar in the paludal zone (3–10 percent plagioclase, <3 percent potassium feldspar) occurs as angular, twinned fragments that have been extensively altered to clay.

Sedimentary lithic fragments constitute a significant fraction (1–9 percent) of the detrital framework grains. Mudstone, siltstone, and shale clasts are most common but often are difficult to recognize because they have been extensively deformed and occur as pseudomatrix. Other lithic constituents include grains of carbonate and rounded, clear to slightly altered fragments of chert (trace to 9 percent). Coal fragments are common in many samples. Detrital carbonate is relatively abundant and occurs as rounded polycrystalline aggregates and partly abraded monocrystalline cleavage fragments that are similar in size to other framework grains. Many rhombohedral grains have an anhedral rim of ankerite that may have formed on the host detrital grain prior to deposition.

Detrital matrix is present but is commonly difficult to differentiate from pseudomatrix. Sandstones containing considerable detrital matrix and pseudomatrix generally show little or no evidence of authigenic mineral cementation or secondary porosity.

Authigenic Minerals

Authigenic minerals in the paludal zone consist of complex intergrowths of ankerite and nonferroan dolomite (3–50 percent) and calcite (trace to 32 percent). Both ankerite and nonferroan dolomite are distributed as pore fill and as replacements of framework grains. They are widespread in sandstones containing detrital dolomite and may have required dolomite nuclei for their growth. Textural relations indicate that much of the ankerite probably formed during late diagenesis.

Authigenic fibrous illite and I/S are the dominant clay minerals in the sandstones. The clay minerals typically occlude pores and probably formed as an alteration product from framework grains (fig. 20).

Reservoir Properties

Porosity and permeability in the paludal zone are variable (<4–>12 percent and <0.1–2.2 mD, respectively). Much of the original porosity was reduced

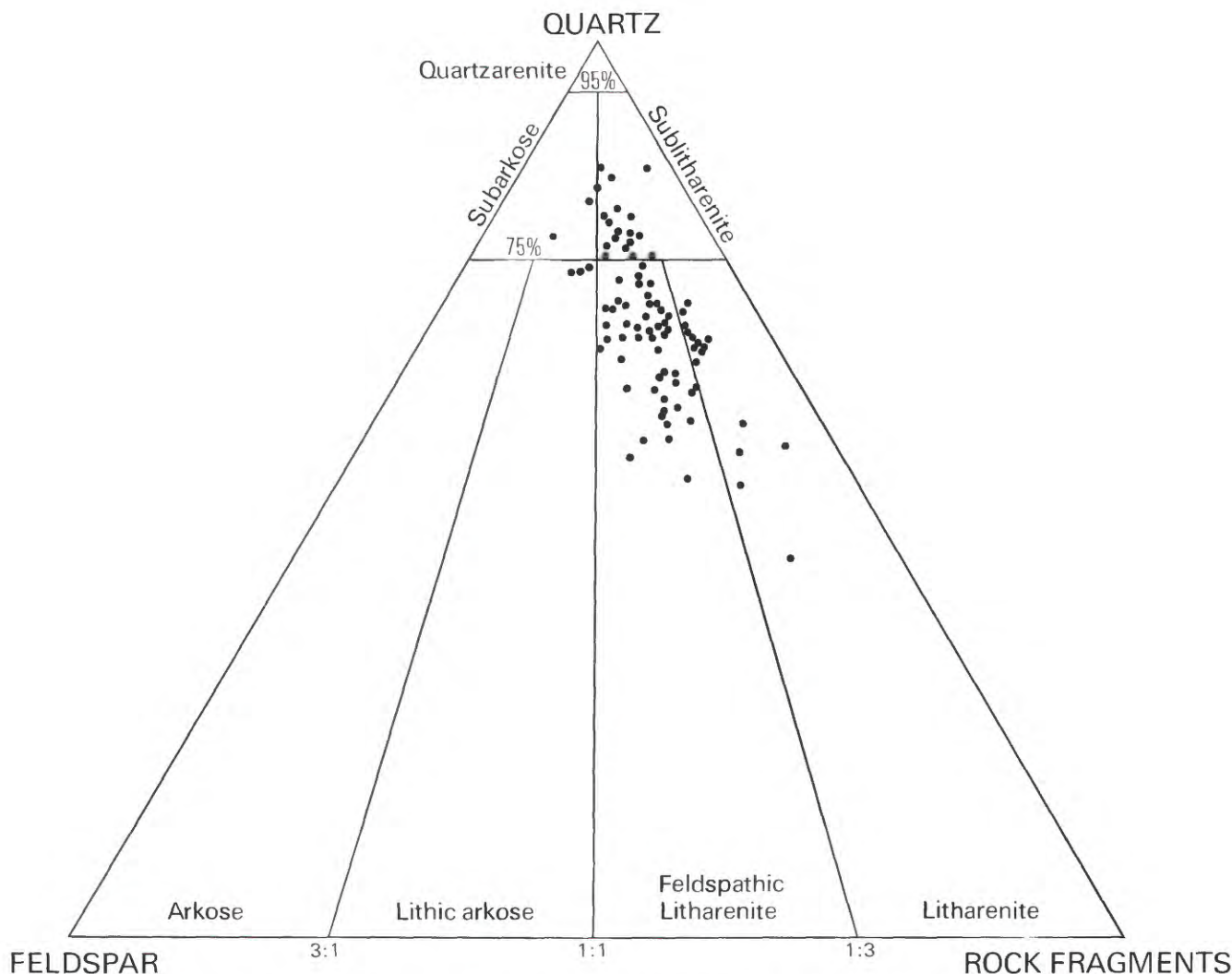


Figure 18. Mineralogic compositions of framework grains in sandstones of paludal zone, MWX wells. Diagram modified from Folk (1974).

by compaction of ductile framework grains during burial. Minor porosity in the sandstones formed from dissolution of lithic fragments. Extensive development of authigenic illite and I/S created a tortuous pore and capillary network in which pore throats commonly are bridged by fibrous clay (fig. 21). This network significantly retards the movement of gas through small capillaries connecting dispersed pores with complex geometries.

Borehole geophysical logs in the paludal zone are particularly difficult to interpret because abundant shale rip-up clasts (fig. 22) cause the reservoir rocks to appear shaly. The presence of these clasts also results in slightly lower than normal (2.68 g/cm^3) grain densities, causes neutron and sonic logs to exhibit anomalously high porosity, and reduces formation resistivity. Coaly grains

in the sandstones commonly increase apparent density- and sonic-log porosity and because of their low density and high resistivity appear as gas saturation. Variable grain density caused by variable amounts of carbonate also complicates interpretation of accurate porosity values from well logs. A crossplot of core-measured grain density and core porosity indicates the lack of a consistent porosity-density relationship (fig. 23). Porosities calculated from geophysical-log responses are influenced by both carbonates (high density, low hydrogen) and coal fragments (low density, low hydrogen); each tends to counteract or modify the effects of the other on density and sonic logs, although not always in a consistent manner.

MWX-1 was initially perforated from 7,076 to 7,110 ft (2,156.8–2,164 m) and from 7,120 to 7,144 ft

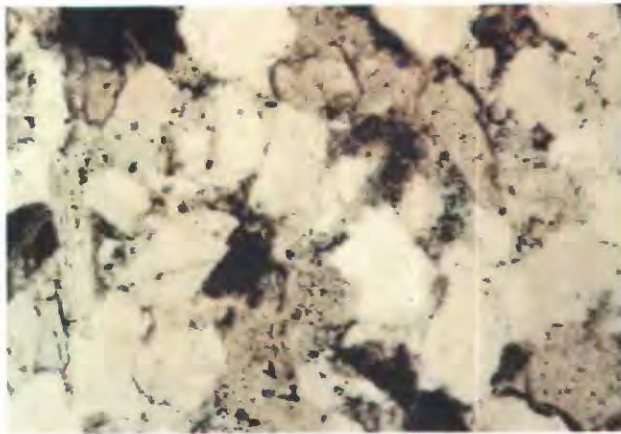
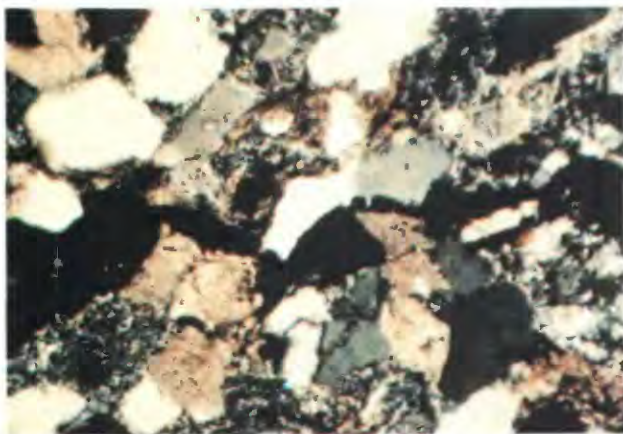


Figure 19. Thin-section photomicrographs showing framework grains and porosity in sandstones of paludal zone, MWX wells. *A*, Detrital grains quartz, feldspar, dolomite, and sedimentary lithic fragments, commonly chert; thin stringer of coaly material (in black). *B*, Low porosity (light blue) in paludal sandstones.

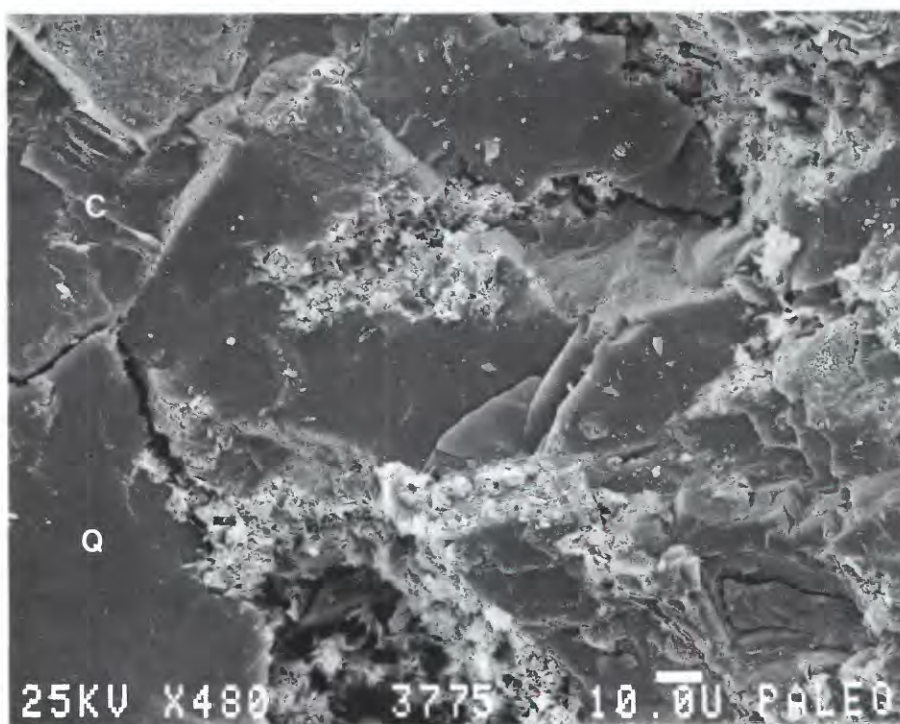


Figure 20. Scanning electron photomicrograph showing framework quartz (Q) and carbonate cement (C) that have been partly dissolved and replaced by authigenic clay in sandstone from paludal zone. Bar scale 10 μ m.

(2,170.2–2,177.5 m). Both intervals were artificially stimulated by using a gel with no proppant (Northrop and others, 1984) in order to determine hydraulic fracture height, length, and orientation using borehole seismic detectors in MWX-2 and MWX-3 (Hart and others,

1984). The height of the induced fracture in these intervals was determined to be about 160 ft (48.8 m) and the one-wing length as far as 375 ft (114.3 m) west-northwest of MWX-1. After initial stimulation, the paludal zone was hydraulically fractured by using 193,000

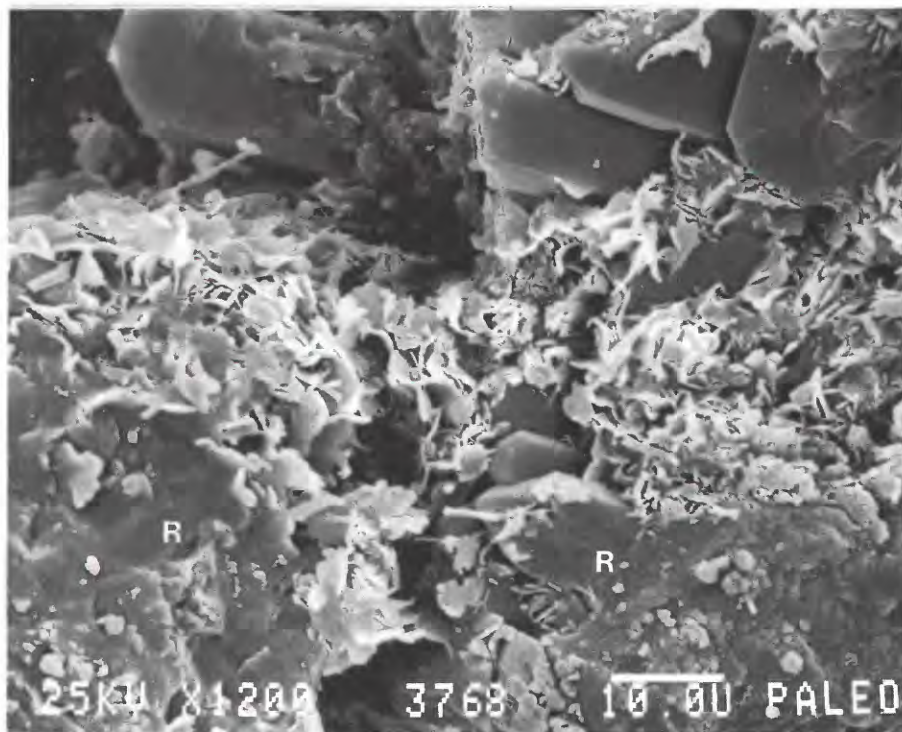


Figure 21. Scanning electron photomicrograph showing illite and illite/smectite replacing rock fragments (R) and bridging pore throats. Bar scale 10 μm .

MWX-7281.6 MWX-7285.3 MWX-7358.0

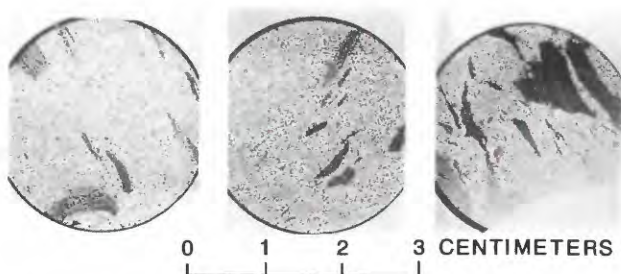


Figure 22. Thin-section photomicrographs showing abundant rip-up shale and siltstone clasts reworked into enclosing sandstone beds in MWX-2 well. Numbers indicate core depths (in feet).

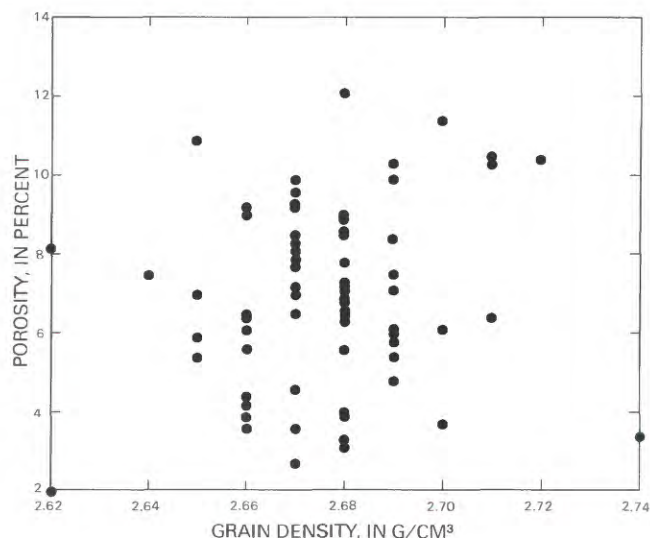


Figure 23. Core porosity and core-measured grain density of sandstones in paludal zone, MWX wells. Nearly random variability caused by shale and siltstone rip-up clasts, coaly fragments, and carbonate minerals.

pounds (87,545 kg) of sand proppant. The prefracture flow rate was about 250,000 cubic feet per day (250 MCFD) and the postfracture flow rate about 170 MCFD; the difference in rates suggests that extensive formation damage may have occurred during fracturing and during fracture-fluid leak-off. The paludal zone was retested after having been shut-in, during testing of the coastal zone, and the flow rate was 300 MCF of gas per day and 30 barrels of water. Although a hydraulic-fracture treatment of this size should have resulted in a flow rate considerably greater than 300 MCFD, both

permeability and reservoir pressure improved during the shut-in period. Modeling of pressure-drawdown and pressure-buildup tests clearly indicates that the intersection of artificial hydraulic fractures and natural fractures within the paludal zone significantly increased

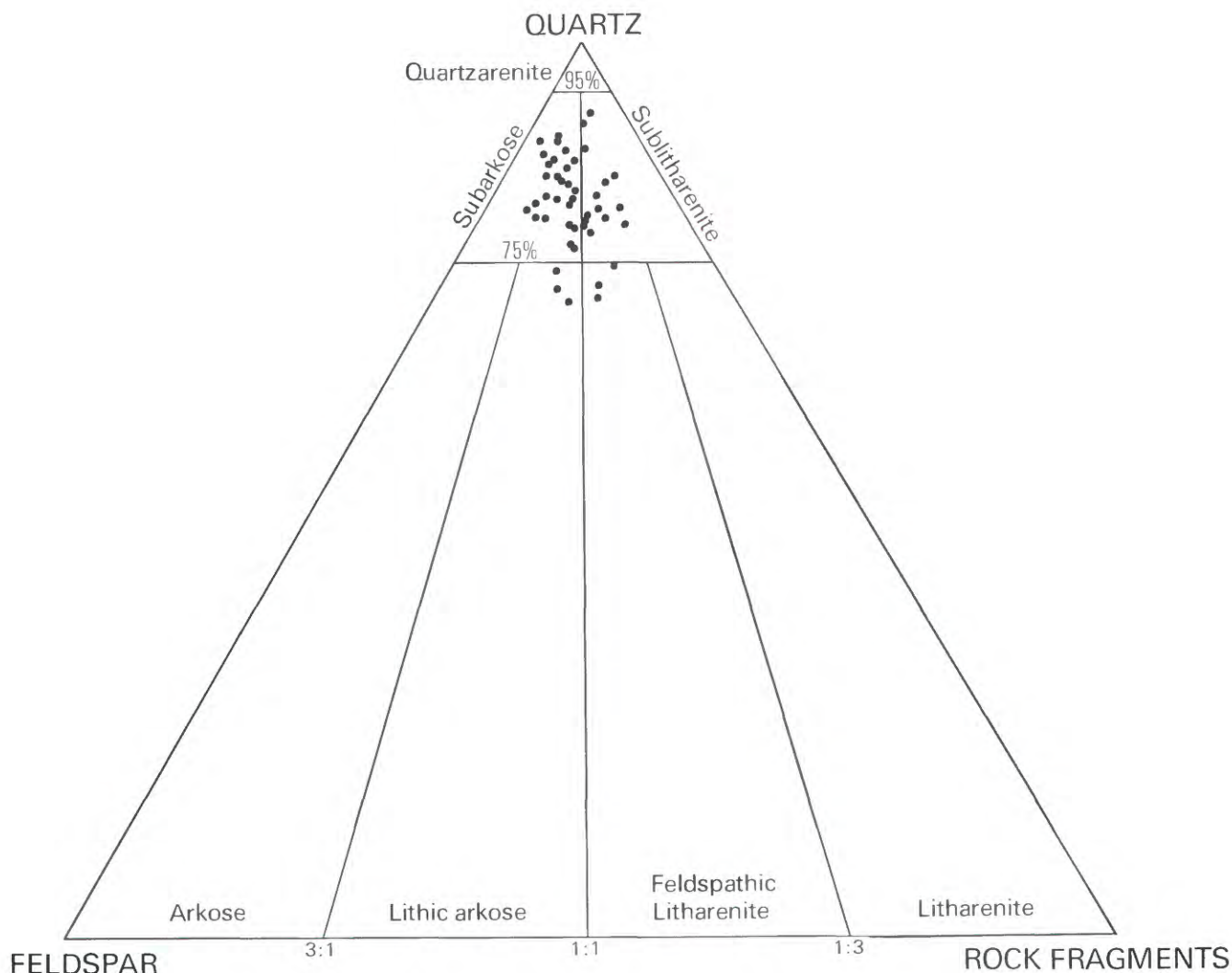


Figure 24. Mineralogic compositions of framework grains in sandstones of shoreline-marine zone, MWX wells. Diagram modified from Folk (1974).

effective reservoir permeability to about 50 mD as compared to 2.3 mD measured on restored-state paludal zone core (Northrop and others, 1984, p. 354).

Shoreline-Marine Zone

The shoreline-marine zone extends from about 7,455 to 8,350 ft (2,272–2,545 m) and is composed of fine-grained, crossbedded, laterally continuous sandstones interbedded with shales and thin coals. Both the sedimentary structures characteristic of a marine environment and the blanket geometry of the sandstones suggest sediments were deposited in a wave-dominated shoreline-delta system (Lorenz, 1982, 1983). Sandstones of the shoreline-marine zone are composed of abundant quartz and lithic fragments and rare plagioclase feldspar. Based on the relative proportions of these constituents,

the sandstones are generally classified as subarkoses (fig. 24). Thin-section photomicrographs of detrital grains, mineral cements, and dissolution features are shown in figure 25.

Framework Grains

Detrital quartz makes up 27–69 percent of the rock and occurs as single monocrystalline grains that are angular to subrounded and very fine to fine in size. Most quartz grains display undulatory extinction, have irregular boundaries, and contain rare inclusions of rutile. They commonly contain abraded overgrowths that suggest recycling from preexisting rock.

Plagioclase and potassium feldspar are minor constituents (2–11 percent and <3 percent, by volume, respectively) and occur either as angular twinned

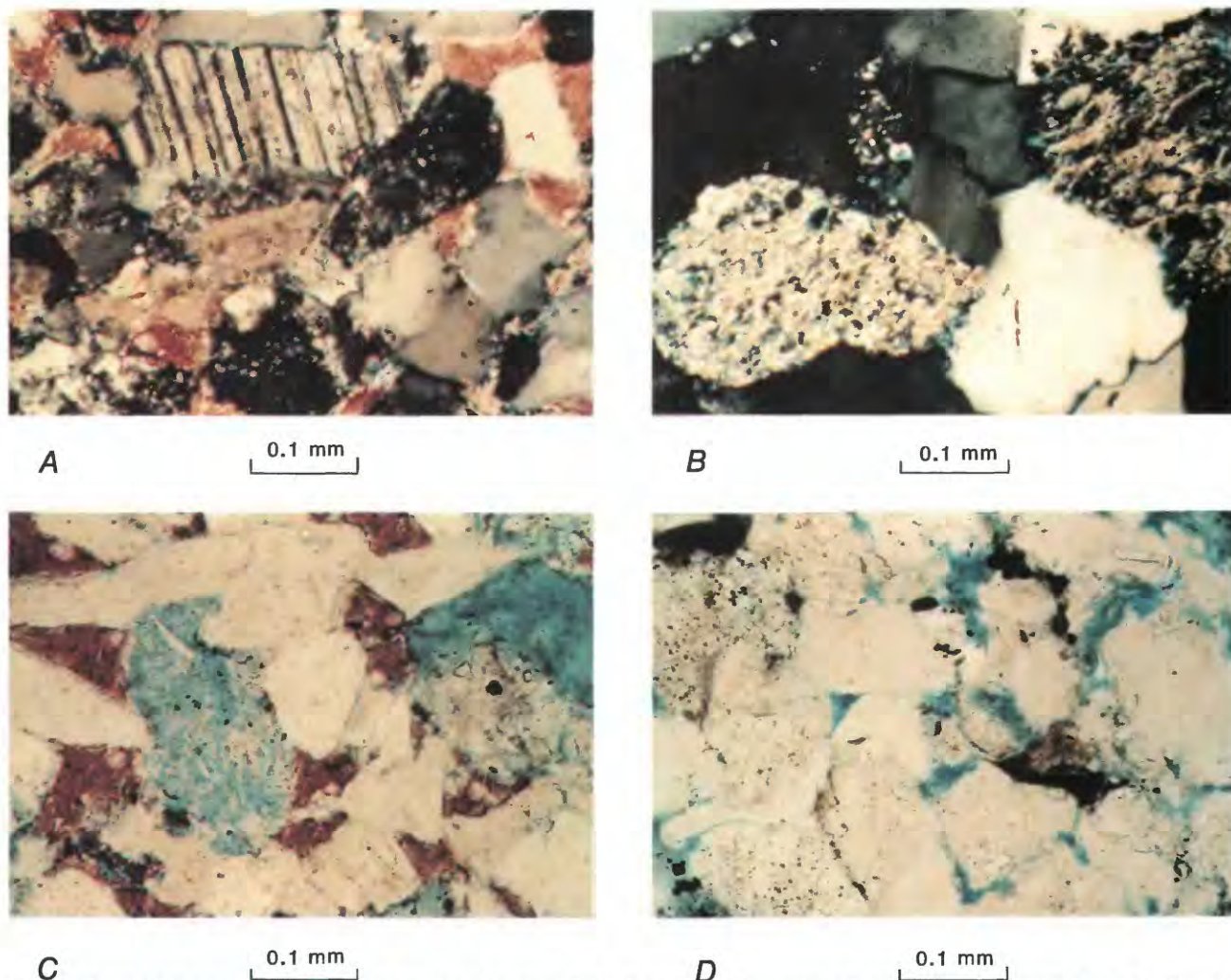


Figure 25. Thin-section photomicrographs showing detrital constituents, mineral cements, and dissolution features in sandstones of shoreline-marine zone, MWX wells. *A*, Detrital quartz, feldspar, and chert. Early generation of calcite (stained red) occurs in pores and replaces grains. *B*, Detrital quartz grains and sericitized sedimentary rock fragments. *C*, Inter- and intragranular secondary porosity (blue). Dissolved grain (center) surrounded by calcite (red) indicates dissolution may have occurred after precipitation of calcite. *D*, Secondary porosity characteristic of Cozzette Sandstone Member.

fragments that are relatively fresh in appearance or as grains that have been altered to clay or sericite.

Sedimentary rock fragments make up 1–8 percent of the rock. Much of the lithic suite is composed of partly dissolved mudstone, clay-rich shale, and siltstone clasts that have been deformed between framework grains to form a pseudomatrix. In sandstones dominated by pseudomatrix, porosity and permeability commonly are considerably reduced. Some sedimentary rock fragments contain sericite.

Chert in the shoreline-marine zone constitutes as much as 5 percent of the rock. Chert grains generally are rounded and composed of microcrystalline interlocking crystals of quartz. Many grains are altered and are light to medium reddish brown; a few grains are almost opaque because of carbonaceous inclusions. Another

variety of chert is relatively unaltered, has unimodal grain size, and is free of inclusions.

Detrital dolomite is present in varying amounts and occurs predominantly as rhombohedral fragments and elliptical polycrystalline aggregates. The size distribution of most dolomite grains is similar to that of nearby framework constituents.

Lithic fragments observed in minor amounts include metamorphic polycrystalline quartz composed of bimodal interlocking crystals that display sutured grain boundaries.

Detrital matrix is common in the sandstones and is similar in appearance to pseudomatrix. The absence of authigenic cement and secondary porosity is probably due to high matrix content.



Figure 26. Scanning electron photomicrograph showing pore containing authigenic iron-rich chlorite. Some individual clay platelets show deformation. Bar scale 10 μ m.

Authigenic Minerals

Authigenic mineral phases include quartz, dolomite (possibly iron bearing), and authigenic illite, I/S and iron-rich chlorite. Secondary silica cement is uncommon because of the large proportion of matrix. Authigenic quartz occurs locally as syntaxial overgrowths in sandstones that contain only minor amounts of matrix material. In these rocks, overgrowths display long to concave-convex contacts; some sutured contacts are observed. Amounts of authigenic calcite (0–21 percent) and dolomite (1–23 percent) are variable. In sandstones in which these minerals are widespread, they replace framework grains and fill pores.

Illite and I/S occur as alteration products of lithic fragments and as pore linings. The relative abundances of both authigenic and detrital clay have significantly reduced porosity and permeability. Figure 26 shows platelets of authigenic chlorite partly filling a pore and replacing an adjacent framework grain. Chlorite was difficult to identify in thin section probably because it is present in relatively small amounts; however, X-ray diffraction analysis reveals strong even-numbered basal reflections that suggest most chlorite is an iron-rich variety (Pollastro, 1984).

Reservoir Properties

The upper and lower parts of the marginal-marine Cozzette Sandstone Member (7,855–7,892 ft, 2,394–2,406 m; 7,940–7,954 ft, 2,420–2,424 m) in the shoreline-marine zone are naturally fractured and contain gas. Porosity in the shoreline-marine zone is 1.6–8.9 percent and probably resulted mostly from dissolution of rock fragments and matrix material (fig. 27). Although some open pores exist between detrital framework grains (fig. 28), most inter- and intragranular pores show extensive authigenic clay-mineral growth. No textural evidence indicates that dissolved framework grains were replaced by carbonate prior to dissolution even in sandstones containing abundant carbonate. A tortuous, disconnected pore network resulting from clay bridges and pore throats filled with clay (fig. 29) and small capillaries has significantly reduced fluid flow, and permeability determined by conventional laboratory techniques is low (<0.01 mD). Permeability to gas at in situ conditions of confining stress and water saturations would be considerably lower. Borehole-log analysis of the marine Corcoran and Cozzette Sandstone Members generally is less complex than that of the overlying nonmarine fluvial sandstone units; however, uncorrected

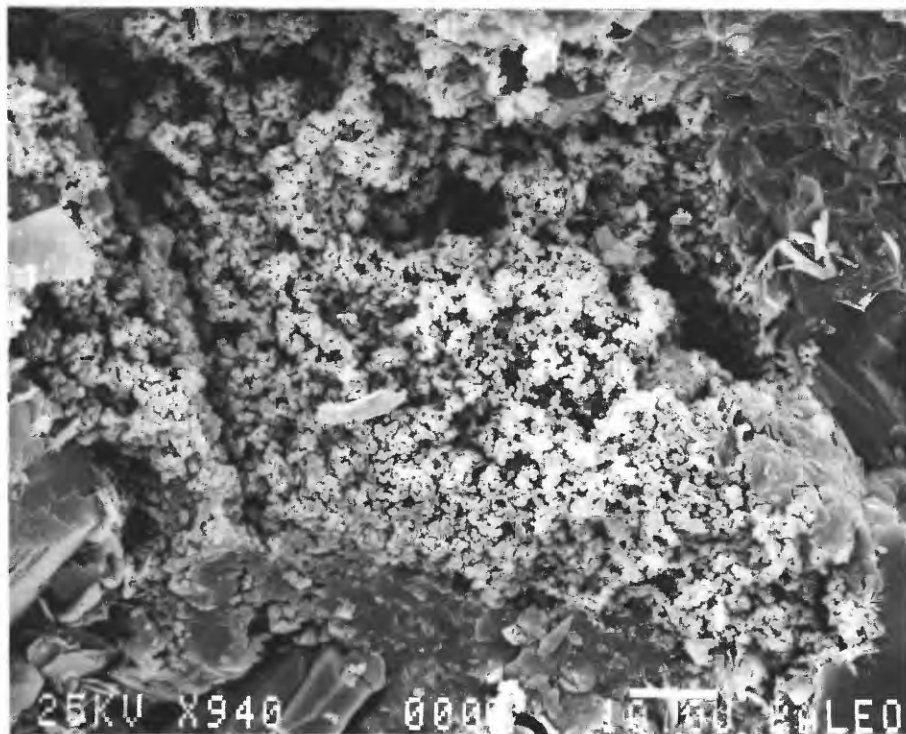


Figure 27. Scanning electron photomicrograph showing microporosity between individual silica crystals in partly dissolved chert grain (center). Bar scale 10 μm .

porosity logs typically yield some anomalously high porosity values similar to those in the fluvial sandstones. These high values can be attributed in part to the presence of matrix clay and rock fragments.

A dark pyrobitumen was observed in the upper cored part of the Cozzette in the 7,824–7,848-ft interval (2,385–2,392 m) of the MWX–2 well (N.H. Bostick, oral commun., 1983). The vitrinite reflectance at this depth is about 2.0 percent (Bostick and Freeman, 1984); a vitrinite reflectance of 1.35 percent generally is considered to be the upper maturation limit for the occurrence of oil. Core porosity in this interval is about 3 percent, whereas porosity of reservoir rocks below this interval is about 8 percent. About 60 percent of the pore space is occupied by bitumen. Although the equivalent interval was not cored in the MWX–1 well, borehole-log analysis indicates that bitumen is present.

Stable isotope and geochemical analyses of gas recovered from the MWX wells indicate that most gas in the Mesaverde was thermally generated from interbedded coals and organic-rich shales (D.D. Rice, written commun., 1982). Gas samples from the paludal and shoreline-marine zones have isotopic and chemical compositions characteristic of marine source rocks; some gas in these intervals probably was generated from organic matter associated with the marine Mancos Shale. This interpretation is consistent with the presence of tongues of Mancos Shale below the paludal zone and

above the Corcoran and Cozzette Sandstone Members. The main part of the Mancos Shale underlies the Corcoran Sandstone Member.

Initial well-to-well interference testing was undertaken in the Cozzette Sandstone Member (MWX–1) to analyze the permeability of marine blanket reservoirs. Because the Cozzette was not a major target for testing, the interval from 7,855 to 7,892 ft (2,394.2–2,405.5 m) was fractured using only 55 barrels of 2 percent potassium chloride water (Branagan and others, 1984, p. 360); no proppant was used. Although the well was swabbed prior to formation fracturing, the unstimulated perforations would not produce gas. This lack of recoverable gas was expected because laboratory tests had shown that at in situ conditions the rock matrix would have a permeability to gas of less than 0.1 mD (Paul Branagan, oral commun., 1984). After the fracturing, gas started flowing in the well at a rate of 320 MCFD and later at rates of more than 1 million cubic feet per day (MMCFD). Flow in MWX–1 was monitored in MWX–2, which was perforated at an equivalent stratigraphic position. The rapid pressure drawdown (less than 2 hours) detected in MWX–2 indicates that the small induced fracture intersected natural fractures near the well bore, and subsequent pulse testing suggests the presence of an orthogonal fracture system in the Cozzette (Branagan and others, 1984, p. 362). Fractures having optimum permeability trend west-northwest, and

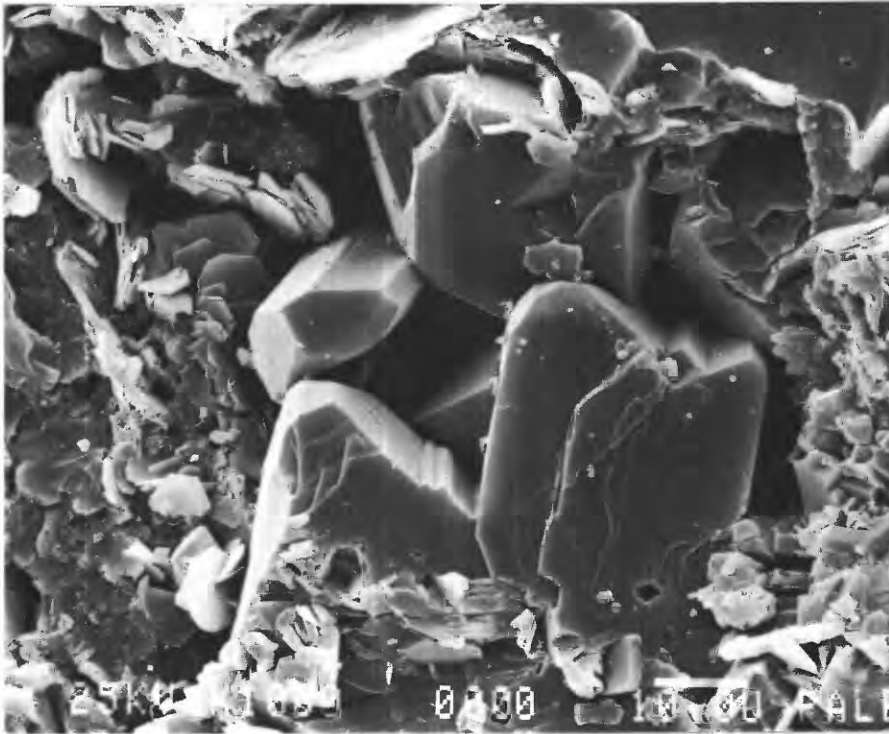


Figure 28. Scanning electron photomicrograph showing open intergranular pores between authigenic quartz crystals (center). Fragments surrounding pores probably are partly dissolved lithic fragments that have been chemically altered to authigenic clay. Bar scale 10 μm .

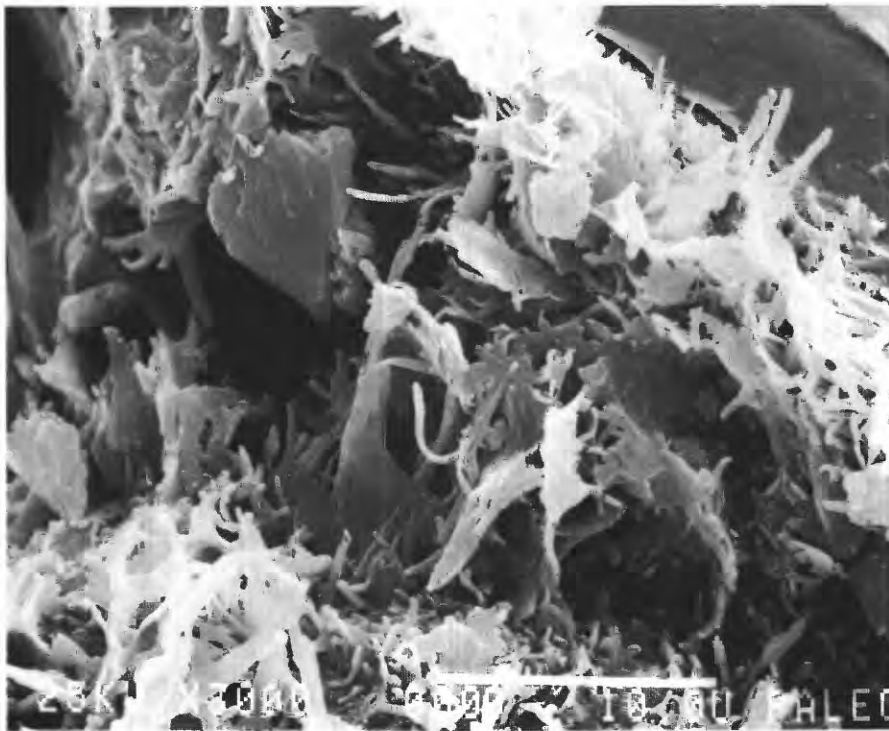


Figure 29. Scanning electron photomicrograph showing fibrous and pore-bridging nature of authigenic illite. Bar scale 10 μm .

a complementary set of fractures having lower permeability trend northeast. On the basis of well testing, the average calculated permeability of the Cozzette interval is from 4 to 7 mD (Branagan and others, 1984, p. 362). The fracture system appears to be continuous within 1,000 ft (305 m) of the well bores.

INTERPRETATIONS FROM CLAY MINERALOGY

Mineral assemblages in sandstones and shales can provide a petrologic and chemical history of both the depositional and diagenetic (postdepositional) environments of the rocks. This history is recorded in both allogenic and authigenic mineral phases, and numerous studies demonstrate depth-dependent mineralogical changes in sedimentary sequences. (See reviews by Weaver, 1979 and Hower, 1981.) Mineral assemblages, in particular clay-mineral assemblages, can be used to determine the extent of diagenesis in the rocks and to evaluate the reservoir quality or source-rock maturity in a potential hydrocarbon province.

The clay-mineral content of representative sandstones from the cored interval of the Mesaverde Group in the MWX wells were determined by XRD. Several sandstones studied, including all samples from the coastal zone, contain only discrete illite and I/S in the clay-size fraction. Abundant authigenic chlorite and kaolinite also occur. Scanning electron microscope analysis reveals that the illite occurs as delicate fibers and laths in pores (fig. 30A), and these fibers commonly bridge pores (fig. 30B). Recognition of discrete fibers of illite is important because they commonly break loose and build up in pore throats during production, reducing permeability and possibly damaging the formation. (See Thomas, 1981, for case studies.)

The composition and ordering of I/S have been used to determine maximum burial temperatures of sedimentary rocks (Hoffman and Hower, 1979; Weaver, 1979; Pollastro and Scholle, 1984; Pollastro and Barker, 1986). In many reservoir sandstones in the MWX wells, I/S occurs as a honeycomblake cement; in most cases it coexists with discrete illite, although the I/S appears to have formed earlier in the burial history (figs. 30C, D). (See Pollastro, 1985, for explanation.) The I/S from the samples analyzed is regularly interstratified (using interpretations from Reynolds and Howar, 1970) and is composed of 75–90 percent illite layers (about 84 percent average; table 2). The shallowest samples (about 4,500 ft, 1,370 m) contain the fewest illite layers in I/S. The increase in the number of illite layers in I/S as depth increases in the MWX wells reflects the increase in temperature with increasing burial depth. Both the high illitic composition and long-range ordering in the I/S

Table 2. Calculated weight percent of clay minerals, <2 μ m fraction, in sandstones and shales, MWX wells

[Sample depth in feet. Lithology: ss, sandstone; sh, shale; (?), uncertain]

| Well number, depth, lithology | Illite (discrete) | Illite/ smectite (I/S) | Chlorite | Kaolinite | Percent illite in I/S |
|----------------------------------|----------------------|------------------------------|----------|-----------|-----------------------------|
| Mixed marine-nonmarine zone | | | | | |
| 1 4454.2 ss | 18 | 37 | 45 | 0 | 75 |
| 1 4499.8 sh | 35 | 49 | 11 | 4 | 78 |
| Fluvial zone | | | | | |
| 3 4909.8 ss | 35 | 50 | 15 | 0 | 80 |
| 3 4926.0 sh | 45 | 45 | 10 | 0 | 82 |
| 3 5820.1 sh | 46 | 19 | 35 | 0 | 86 |
| 3 5840.2 ss | 41 | 28 | 31 | 0 | 84 |
| Coastal zone | | | | | |
| 3 6517.4 ss | 60 | 40 | 0 | 0 | 83 |
| 3 6526.8 sh | 64 | 36 | 0 | 0 | 83 |
| 1 6546.3 ss? | 63 | 37 | 0 | 0 | 86 |
| 1 6556.1 sh? | 60 | 40 | 0 | 0 | 86 |
| Paludal zone | | | | | |
| 3 7101.4 ss | 64 | 36 | 0 | 0 | 88 |
| 3 7114.4 sh | 76 | 24 | 0 | 0 | 88 |
| 2 7105.2 sh | 59 | 41 | 0 | 0 | 88 |
| 2 7124.2 ss | 63 | 37 | 0 | 0 | 90 |
| Shoreline-marine zone | | | | | |
| 2 7826.0 sh | 42 | 49 | 9 | 0 | 87 |
| 2 7854.4 ss | 45 | 44 | 11 | 0 | 85 |

suggest these rocks have experienced deep-burial and high-temperature conditions. The model of Hoffman and Hower (1979) indicates that maximum burial temperatures of approximately 170–180 °C were attained in Cretaceous rocks of the MWX wells (Pollastro, 1984). These paleotemperatures are in good agreement with maximum temperatures calculated by using vitrinite reflectance (Bostick and Freeman, 1984).

Iron chlorite is a common clay mineral in reservoir sandstones in the paludal, fluvial, and shoreline-marine zones. It is extremely fine grained, usually 1 μ m or less in size, and occurs as an authigenic cement or pore linings

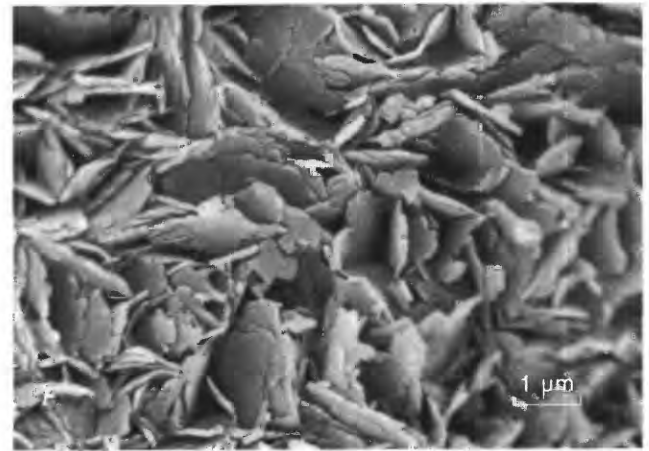
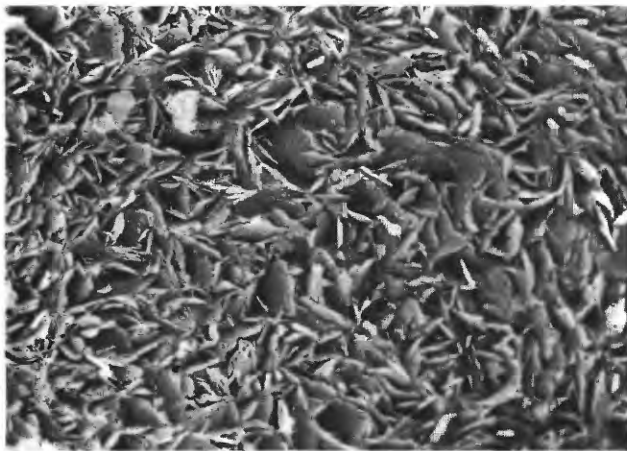
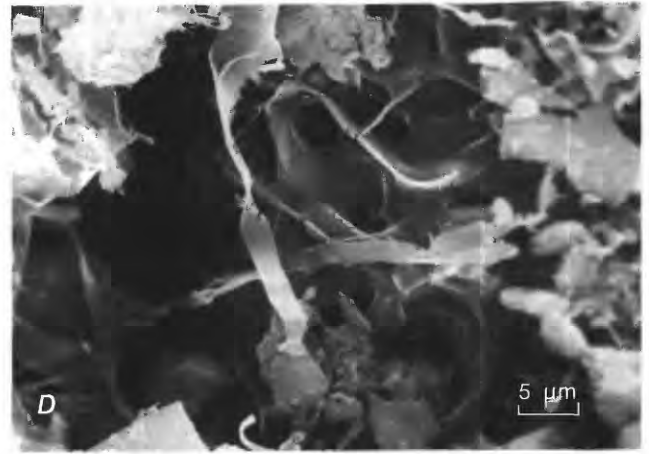
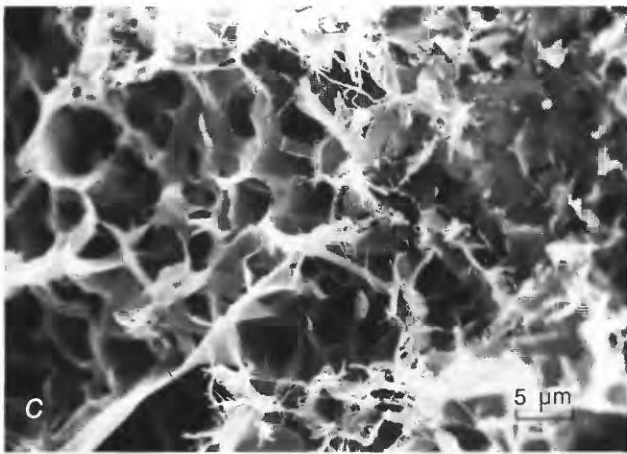
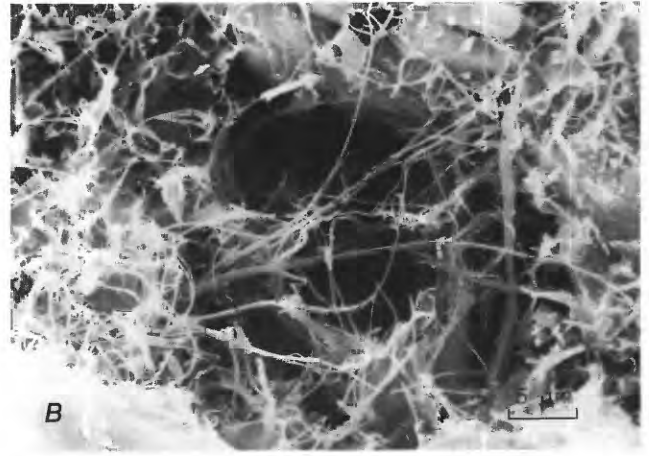
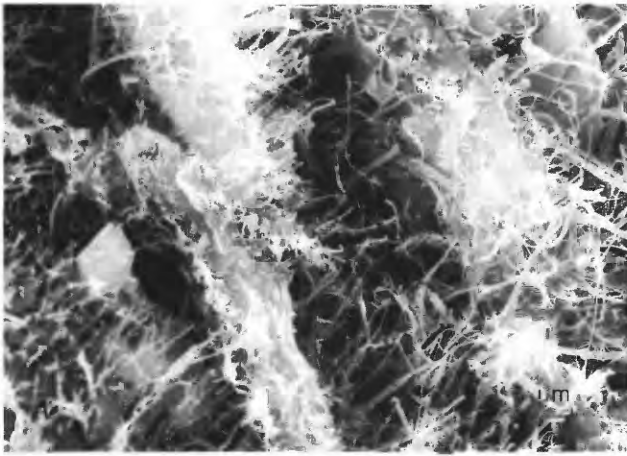


Figure 30. Scanning electron photomicrographs showing clays and cements in sandstones, MWX wells. *A, B*, Fibrous illite. *C, D*, Mixed-layer illite/smectite cement with illite fibers. *E, F*, Fine-grained, iron-rich chlorite cement.

(figs. 30E, F). It commonly creates problems during stimulation and production because it is soluble in acid (in particular, hydrochloric acid) and can easily form iron gels that damage the formation (Thomas, 1981). Some chlorite in the sandstones may be detrital in origin, inasmuch as shale samples that contain presumably detrital, abundant clay also contain chlorite. (For example, see MWX-3 shale sample 4,926.0 ft, table 2.)

X-ray diffraction data (table 2) indicate that if iron chlorite is in a sandstone, it is also in the companion shale. Likewise, if only discrete illite and I/S are in a sandstone, only these clay minerals are found in the paired shale. This similarity between the clay mineralogy, when identified, of a discrete sandstone and that of the adjacent shale may be useful in interpreting log characteristics of these two lithologies in the MWX wells, such as the extrapolation of shaliness factors based on clay mineralogy in potential sandstone reservoirs by using the log response of adjacent shales.

SUMMARY

Major gas resources are present in low-permeability reservoir rocks of Cretaceous age in the Piceance basin, Colorado. Extensive cores and geophysical logs in the MWX wells provide valuable mineralogic and petrophysical data for understanding the factors controlling the reservoir characteristics of low-permeability rocks in complex marine and nonmarine fluvial depositional systems. Petrographic and X-ray diffraction analysis of the cored part of the Upper Cretaceous Mesaverde Group indicate a mineral assemblage consisting of framework quartz, feldspar, volcanic and sedimentary lithic grains, authigenic carbonate minerals including calcite, dolomite and ankerite, and a variety of clays including kaolinite, chlorite, I/S and illite. The abundance, distribution, and grain density of these minerals all significantly affect the reservoir quality of the sandstones. Geophysical logs currently in use were designed and calibrated for conventional reservoirs and often do not accurately reflect reservoir properties that characterize low-permeability rocks (Kukul and others, 1983). Differences in sandstone composition may significantly influence well-log responses and, as a result, porosity and permeability determinations. Alternative log computation methods for predicting reservoir quality in unconventional rocks have recently been described by Kukul (1984).

Core permeabilities in conjunction with permeabilities derived from flow rates and pressure-drawdown and -buildup tests indicate that *all* reservoirs that have been production tested in Cretaceous rocks in the MWX wells are naturally fractured. Analysis of natural fractures and prediction of the orientation of induced hydraulic fractures involves integration of regional tectonics,

surface fracture mapping, stress history, rock mechanics, geophysics, core study, borehole well-log analysis, well testing, and fracture diagnostics. Interpretation of porosity and water saturation values in fractured zones by using borehole geophysical logs requires integration of laboratory-measured core values and petrographic, petrologic and stratigraphic data.

REFERENCES CITED

- Bostick, N.H., and Freeman, V.L., 1984, Tests of vitrinite reflectance and paleotemperature models at the Multiwell Experiment site, Piceance Creek basin, Colorado, in Spencer, C.W., and Keighin, C.W., eds., *Geologic studies in support of the U.S. Department of Energy Multiwell Experiment, Garfield County, Colorado: U.S. Geological Survey Open-File Report 84-757*, p. 110-120.
- Branagan, P., Cotner, G., and Lee, S.J., 1984, Interference testing of naturally fractured Cozzette Sandstone; a case study at the DOE MWX site: *Society of Petroleum Engineers/Gas Research Institute/U.S. Department of Energy Unconventional Gas Recovery Symposium, Pittsburgh, Pa., 1984, Proceedings*, p. 359-366.
- Dunn, H.L., 1974, *Geology of petroleum in the Piceance Creek basin, northwestern Colorado: Rocky Mountain Association of Geologists Field Conference, Guidebook 25*, p. 217-224.
- Folk, R.L., 1974, *Petrology of sedimentary rocks*: Austin, Tex., Hemphill, 182 p.
- Hart, C.M., Engi, D., Fleming, R.P., and Morris, H.E., 1984, Fracture diagnostics results for the multiwell experiment's paludal zone stimulations: *Society of Petroleum Engineers/Gas Research Institute/U.S. Department of Energy Unconventional Gas Recovery Symposium, Pittsburgh, Pa., 1984, Proceedings*, p. 221-228.
- Hoffman, J., and Hower, J., 1979, Clay mineral assemblages as low grade metamorphic geothermometers; application to the thrust faulted disturbed belt of Montana, U.S.A., in Scholle, P.A., and Schluger, P.K., eds., *Aspects of diagenesis: Society of Economic Paleontologists and Mineralogists Special Publication 26*, p. 55-79.
- Hower, J., 1981, Shale diagenesis, in Longstaffe, F.J., ed., *Clays and the resource geologist: Mineralogical Association of Canada Short Course Handbook 7*, p. 60-80.
- Johnson, R.C., 1988, Geologic history and hydrocarbon potential of Late Cretaceous-age, low-permeability reservoirs, Piceance basin, western Colo.: *U.S. Geological Survey Bulletin 1787-E*, in press.
- Kukul, G.C., 1984, A systematic approach for effective log analysis of tight gas sands: *Society of Petroleum Engineers/Gas Research Institute/U.S. Department of Energy Unconventional Gas Recovery Symposium, Pittsburgh, Pa., 1984, Proceedings*, p. 209-220.
- Kukul, G.C., Biddison, C.L., Hill, R.E., Monson, E.R., and Simons, K.E., 1983, Critical problems hindering accurate log interpretation of tight gas reservoirs: *Society of Petroleum Engineers/U.S. Department of Energy Joint*

- Symposium on Low Permeability Gas Reservoirs, Denver, Colo., 1983, Proceedings, p. 181-190.
- Lorenz, J.C., 1982, Sedimentology of the Mesaverde Formation at Rifle Gap, Colorado, and implications for gas-bearing intervals in the subsurface: Albuquerque, N. Mex., Sandia National Laboratories Report SAND82-0604, 44 p.
- 1983, Reservoir sedimentology in Mesaverde rocks at the Multi-Well Experiment site: Albuquerque, N. Mex., Sandia National Laboratories Report SAND83-1078, 33 p.
- Mann, R.L., 1984, Multiwell Experiment drilling review, in Fohne, K-H., ed., Western gas sands subprogram review, technical proceedings: U.S. Department of Energy DOE/METC/84-3, p. 155-164.
- National Petroleum Council, 1980, Tight gas reservoirs; part I, in National Petroleum Council unconventional gas resources: Washington, D.C., National Petroleum Council, 222 p.
- Northrop, D.A., ed., 1985, Second technical poster session for the Multiwell Experiment: Society of Petroleum Engineers/U.S. Department of Energy Symposium on Low Permeability Reservoirs, Albuquerque, N. Mex., Sandia National Laboratories Report SAND86-0945, 84 p.
- Northrop, D.A., Sattler, A.R., Mann, R.L., and Frohne, K-H., 1984, Current status of the Multiwell Experiment: Society of Petroleum Engineers/Gas Research Institute/U.S. Department of Energy Unconventional Gas Recovery Symposium, Pittsburgh, Pa., 1984, Proceedings, p. 351-358.
- Pitman, J.K., and Sprunt, E.S., 1986, Origin and distribution of fractures in lower Tertiary and Upper Cretaceous rocks, Piceance basin, Colorado, and their relation to the occurrence of hydrocarbons: American Association of Petroleum Geologists Studies in Geology 24, p. 221-234.
- Pollastro, R.M., 1984, Mineralogy of selected sandstone/shale pairs and sandstone from the Multiwell Experiment; interpretations from X-ray diffraction and scanning electron microscopy analyses, in Spencer, C.W., and Keighin, C.W., Geologic studies in support of the U.S. Department of Energy Multiwell Experiment, Garfield County, Colorado: U.S. Geological Survey Open-File Report 84-757, p. 67-74.
- 1985, Mineralogical and morphological evidence for the formation of illite at the expense of illite/smectite: Clays and Clay Minerals, v. 33, p. 265-274.
- Pollastro, R.M., and Barker, C.E., 1986, Application of clay-mineral, vitrinite reflectance, and fluid inclusion studies to the thermal and burial history of the Pinedale anticline, Green River basin, Wyoming, in Gautier, D.L., ed., Roles of organic matter in sediment diagenesis: Society of Economic Paleontologists and Mineralogists Special Publication 38, p. 73-83.
- Pollastro, R.M., and Scholle, P.A., 1984, Hydrocarbons exploration, development from low-permeability chalks, Upper Cretaceous Niobrara Formation, Rocky Mountains region: Oil and Gas Journal, v. 82, no. 17, p. 140-145.
- Reynolds, R.C., Jr., and Hower, J., The nature of interlayering in mixed-layer illite-montmorillonites: Clays and Clay Minerals, v. 18, no. 1, p. 25-36.
- Sattler, A.R., 1984, The Multiwell Experiment core program: Society of Petroleum Engineers/U.S. Department of Energy/Gas Research Institute Unconventional Gas Recovery Symposium, Dallas, Tex., 1984, Proceedings, p. 235-244.
- Scanlon, A.H., 1983, Oil and gas field map of Colorado: Colorado Geological Survey Map Series 22, scale 1:500,000.
- Spencer, C.W., 1984, Overview of U.S. Department of Energy Multiwell Experiment, Piceance Creek basin, Colorado, in Spencer, C.W., and Keighin, C.W., eds., Geologic studies in support of U.S. Department of Energy Multiwell Experiment, Garfield County, Colorado: U.S. Geological Survey Open-File Report 84-757, p. 1-13.
- 1985, Geologic aspects of tight gas reservoirs in the Rocky Mountain region: Journal of Petroleum Technology, v. 37, no. 8, p. 1308-1314.
- 1987, Hydrocarbon generation as a mechanism for overpressuring in Rocky Mountain region: American Association of Petroleum Geologists Bulletin, v. 71, no. 4, p. 368-388.
- Thomas, J.B., 1981, Classification and diagenesis of clay minerals in tight gas sandstones; case studies in which clay mineral properties are crucial to drilling fluid selection, formation evaluation, and completion techniques, in Longstaffe, F.J., ed., Clays and the resource geologist: Mineralogical Association of Canada Short Course Handbook 7, p. 104-118.
- Weaver, C.E., 1979, Geothermal alteration of clay minerals and shales; diagenesis: Office of Nuclear Waste and Isolation Technical Report 21, 176 p.
- Young, R.G., 1982, Stratigraphy and petroleum geology of the Mesaverde Group, southeastern Piceance Creek basin, Colorado: Grand Junction Geological Society Guidebook, p. 45-54.

